Cleaner Engineering and Technology 13 (2023) 100629

Contents lists available at ScienceDirect

Cleaner Engineering and Technology

journal homepage: www.sciencedirect.com/journal/cleaner-engineering-and-technology

Application of machine learning algorithm in the internal and external hazards from industrial byproducts

Solomon Oyebisi [a,*], Hilary Owamah [b], Maxwell Omeje [c]

[a] Department of Civil Engineering, Covenant University, PMB 1023, Km 10, Idiroko Road, Ota, Nigeria
[b] Department of Civil and Environmental Engineering, Delta State University, Abraka, Nigeria
[c] Department of Physics, Covenant University, PMB 1023, Km 10, Idiroko Road, Ota, Nigeria

ARTICLE INFO

Keywords:
Cleaner production
Machine learning algorithm
Recycling
Responsible consumption and production
Waste valorization

ABSTRACT

Natural radioactive substances that are produced because of industrial processes pose a risk to both the environment and people. An extensive analysis of the radiological properties of industrial byproducts was undertaken in this work, and the risks for both indoor and outdoor environments were assessed based on activity concentrations. The machine learning technique of artificial neural networks was used with various training algorithms to predict the internal and external hazards from these industrial byproducts. The findings demonstrated that, with the exception of incinerated sewage sludge ash, metakaolin, marble powder, nickel slag, pyrite ash, silica fume, steel slag, and glass waste powder, every industrial byproduct examined poses potential indoor and outdoor dangers. All backpropagation training algorithms that were used showed high prediction, according to the neural networks. However, when compared to the Bayesian Regularization and Scaled Conjugate Gradient backpropagation training algorithms, the Levenberg-Marquardt backpropagation technique had the best performance indicators for training, validation, and testing. The results can provide reference information for developing a framework for monitoring hazards and their accompanying precise management.

1. Introduction

A growing population has accelerated urbanization and industrialization, forcing the manufacturing industries to produce more and new materials to keep up with demand (Sharma et al., 2022). Due to their improper management and indiscriminate disposal, the production of industrial products generates a variety of solid wastes that pose problems for society and the environment (Gaur et al., 2020; Kundariya et al., 2021). In order to manage and recycle these wastes as useful goods, a concerted effort has been made. Because of this, industrial byproducts - recycled goods made from industrial waste - have been held up as models for delivering advantages to the society, environment, the economy, and products (Schaubroeck et al., 2021; United States Environmental Protection Agency, 2008). This idea has gained more popularity and is now being used to partially or completely replace cement (Aprianti et al., 2015; Mora et al., 2016). Industrial byproducts used as additives for cement and concrete manufacture include slag and fly ash. Others are granite waste powder, silica fume, volcanic ash, bottom ash, red mud, metakaolin (Alonso et al., 2020; Aprianti et al., 2015; Oyebisi et al., 2020a, 2020b; Sas et al., 2019). According to Gaur et al. (2020), recycling or valorizing industrial waste offers a practical strategy to cut waste while creating economic value, resulting in a sustainable approach to waste treatment. However, the majority of industrial wastes are said to be technologically enhanced naturally occurring radioactive materials (TENORM), which in small quantities can be hazardous to both human health and the environment (Imani et al., 2021; Kovler, 2012; United Nations Scientific Committee on the Effects of Atomic Radiation, 2000; United States Environmental Protection Agency, 2022). Aside from that, prior research has demonstrated that industrial wastes are hazardous to both the environment and human health (Gaur et al., 2020; Kundariya et al., 2021; MandeepKumar Gupta and Shukla, 2020; Ravindran et al., 2018).

Natural radionuclides (NORs) like the potassium (^{40}K) isotope, thorium (^{232}Th) and uranium/radium (^{238}U/^{226}Ra) series are the primary sources of radiation in industrial byproducts (Council of European Union, 2014; Kovler, 2012; United Nations Scientific Committee on the Effects of Atomic Radiation, 2000). This is demonstrated by similar studies that ^{226}Ra, ^{232}Th, and ^{40}K in building and construction materials are the main sources of human exposure (Kocsis et al., 2021; Mehra et al., 2010; Sas et al., 2019). However, prolonged exposure to radium

* Corresponding author.
E-mail address: solomon.oyebisi@covenantuniversity.edu.ng (S. Oyebisi).

https://doi.org/10.1016/j.clet.2023.100629
Received 5 February 2023; Received in revised form 14 March 2023; Accepted 2 April 2023
Available online 4 April 2023

and thorium isotopes can increase the risk of bone, liver, or breast cancer through ingestion, lacerations, feces, and urine (United Nations Scientific Committee on the Effects of Atomic Radiation, 1993; World Health Organization, 2009). More than 85% of people on the planet are exposed to radiation from ^{226}Ra, ^{232}Th, and ^{40}K's short-lived offspring radionuclides. These radionuclides, in the built environment, continually decay (Joel et al., 2019; Maxwell et al., 2015; United Nations Scientific Committee on the Effects of Atomic Radiation, 2008; 2000, 1993).

Sanjuán (2022) examined the radioactive concentration of industrial byproducts (coal slag) utilized as building material. The findings indicated the existence of radionuclides with harmful effects on health. The radioactivity of building materials from the Campania region, including tuff, pumice, and others, was investigated by Sabbarese et al. (2021). The findings demonstrated that building materials' radioactive content is dependent on the geological settings and features, with volcanic rock samples having a higher radioactive concentration than carbonate rock. Therefore, materials derived from volcanic rock sources faced radioactive health concerns. An environmental impact of the radiological hazard of phosphogypsum (industrial byproduct) was assessed by researchers (Narloch et al., 2019; Qamouche et al., 2020). Due to the higher concentrations of ^{226}Ra and ^{40}K, the findings demonstrated that the calculated internal and external risks in phosphogypsum were more than the world population-weighted average value of 1, posing environmental and health risks. Nevertheless, despite several studies on the radioactivity of industrial byproducts, there is no reflection on the thorough details and machine learning-based modeling of alpha and gamma radiation of industrial byproducts used as building and construction materials; this is why this study was conducted.

The trend of applying machine learning techniques to forecast the properties of materials has gotten a lot of attention recently. It contains unique algorithms that can learn from data and present more accurate findings as output data in comparison to conventional regression approaches (Ley and Bordas, 2018; P. Lu et al., 2012; Salehi and Burgueño, 2018). It uses techniques and models developed from statistics and probability theory rather than symbolic approaches (Langley, 2011). In fact, by studying a sufficient number of data samples, machine learning algorithms (MLA) enable machines to learn the information they require to carry out a certain task (Dietterich, 2000; Ghahramani, 2015). Prior to using the algorithm, a process known as feature extraction must be completed, in which the attributes that best describe the most specific data are extracted. The sample data used in the process stage, which trains the system to transmit characteristics and distinguish patterns, is based on a particular machine learning training technique (Avci et al., 2021; Haenlein and Kaplan, 2019; Marani and Nehdi, 2020). Machine learning has been engaged in structural engineering in a number of areas, including the evaluation of seismic performance (Liu et al., 2020), identification of structural systems (Jiang et al., 2007), and vibration control (Abdeljaber et al., 2016), modeling of strengths (Dutta and Barai, 2019; Pazouki, 2022; Wang et al., 2022; Yeh, 1998; Ziolkowski and Niedostatkiewicz, 2019), to mention a few. The use of MLA in medicine, which is highly accurate and uses a dataset with intricate reports, is another crucial feature of the MLA (İnce et al., 2022; Olthof et al., 2021). Although there has been a lot of research on the use of MLA, no study has used this technology to predict internal and external hazards from industrial byproducts.

This study offers a thorough analysis of industrial byproducts, focusing on their activity concentrations to measure the internal and external hazards. The artificial neural networks (ANN) of supervised machine learning algorithms were used to train the hazard data using Bayesian Regularization, Scaled Conjugate Gradient, and the Levenberg-Marquardt training algorithm. The most effective algorithm for predicting internal and external hazards was found by contrasting the metrics of each technique's effectiveness. These results support the identification and prediction of hazards to people who dwell in buildings produced with these byproducts. Additionally, it offers the reference information needed to create a framework for monitoring indoor and outdoor hazards.

2. Methodology adopted for review and data source and collection

The process includes obtaining, screening, and assessing pertinent materials. A dataset was located using a number of databases, including Science Direct, Web of Science, and Google Scholar. To maximize data collection, pertinent information was also gathered from UNSCEAR, WHO, CEU, European Commission (EC), and the Canadian Nuclear Safety Commission (CNSC). Others included the Organization for Economic Co-operation and Development (OECD), International Atomic Energy Agency (IAEA), and International Commission on Radiological Protection (ICRP) (NEA-OECD). As the concept of naturally occurring radioactive in building and construction materials spreads, several studies are available. Using keywords such as 'naturally occurring radioactive materials,' 'building materials,' 'construction materials,' 'machine learning algorithms,' and 'supplementary cementitious materials,' 1383 papers were found during the initial search. The search engine was further broadened to include terms such as 'industrial byproducts' and 'internal and external hazards of industrial wastes' due to the study's emphasis on applying machine learning algorithms to predict the internal and external hazards from industrial byproducts. Finally, 517 publications representing the papers remained. Only peer-reviewed publications were taken into account to maintain the high quality of the review (Chinnu et al., 2021). The significance of the study was taken into consideration when screening, with a focus on the activity concentrations (^{226}Ra, ^{232}Th, and ^{40}K) of industrial byproducts. The literature was further improved based on removing extraneous information, adding papers on internal and external hazards of building and construction materials, excluding publications on agricultural byproducts, and excluding articles on machine learning algorithms other than supervised learning approaches.

By creating targeted inquiries based on the main subject of the current study, new screening methods were created. The following standards are taken into consideration by the strategies: Are the articles primarily focused on the radioactivity of industrial byproducts? In the publications surveyed, what categories of activity concentrations are examined? Is the primary focus of the literature internal and external hazards of industrial byproducts? Which relationship was used globally to calculate the internal and external hazards of building and construction materials? Does each article predict the outcomes using a specific MLA?

After screening, a sample size of 234 applicable peer-reviewed papers was obtained. These papers were investigated, validated, and controlled by methodically individuating, researching, examining, and reading the publications and references. After careful consideration, 172 extremely relevant journals were selected for the study.

3. Hazard indexes

The radiation dose for safe building materials is 1 mSv y^{-1} for internal and external radiation hazard indexes (Beretka and Mathew, 1985; Hassan et al., 2010; Kasumović et al., 2018; Ravisankar et al., 2012).

3.1. Internal hazard index (H_{in})

Thoron and radon, two short-lived isotopes, release alpha particles together with gamma rays of various energies. This is known as the internal hazard index. The internal radiation hazard index measures the amount of excess internal alpha radiation that is intrinsically exposed as a result of breathing in ^{222}Rn and its short-lived offspring produced by industrial byproducts (Beretka and Mathew, 1985; Gökçe et al., 2020; Imani et al., 2021; United Nations Scientific Committee on the Effects of Atomic Radiation, 2000; 1993). The index of internal hazard should be

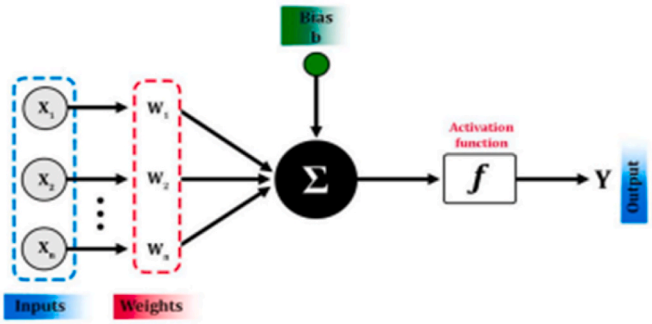

Fig. 1. The architecture of ANN (Mohtasham Moein et al., 2023).

less than unity, as illustrated in Eq. (1), to make the radiation hazard insignificant (Caridi et al., 2021; El-Bahi et al., 2017; Stoulos et al., 2003; United Nations Scientific Committee on the Effects of Atomic Radiation, 2000; 1993):

$$H_{in} = \left(\frac{A_{Ra}}{185Bq\ kg^{-1}} + \frac{A_{Th}}{259Bq\ kg^{-1}} + \frac{A_K}{4810Bq\ kg^{-1}}\right) \leq 1 \quad (1)$$

3.2. External hazard index (H_{ex})

Another metric for determining whether NORs of materials are appropriate is external radiation hazard (Ravisankar et al., 2012). Due to the naturally occurring radionuclides in building materials, external exposure to terrestrial gamma radiation creates a radiation hazard (Gökçe et al., 2020; United Nations Scientific Committee on the Effects of Atomic Radiation, 2000). The radiation hazard is negligible because H_{ex} is allowed to have a limit below unity. In order to use building materials safely, this value equates ^{226}Ra, ^{232}Th, and ^{40}K to upper limit of 370, 259, and 4810 Bq kg-1, respectively (Imani et al., 2021; Legasu and Chaubey, 2022; Shoeib and Thabayneh, 2014; United Nations Scientific Committee on the Effects of Atomic Radiation, 2000; 1993). However, if the external radiation hazard index is more than one, the potential external dosage to the exposed population could be higher than the safe level, which could represent a health risk (Beretka and Mathew, 1985; Imani et al., 2021). Hence, the external radiation hazard index (H_{ex}) is determined following Eq. (2):

$$H_{ex} = \left(\frac{A_{Ra}}{370Bq\ kg^{-1}} + \frac{A_{Th}}{259Bq\ kg^{-1}} + \frac{A_K}{4810Bq\ kg^{-1}}\right) \leq 1 \quad (2)$$

where A_{Ra}, A_{Th}, and A_K are activity concentrations of ^{226}Ra, ^{232}Th, and ^{40}K, respectively (Bq kg^{-1}).

4. Machine learning algorithm

This study employs a machine learning approach because it has produced highly precise models for a significant number of published articles on the manufacture of concrete that contains industrial byproducts(Asadi Shamsabadi et al., 2022; Baduge et al., 2022; Naseri et al., 2020; Nguyen et al., 2020, 2021). A machine learning algorithm completes a given task, learns input parameters without explicit programming, and provides an accurate forecast or outcome (Kim, 2017). The artificial neural network (ANN) of machine learning algorithms was engaged using MATLAB R2021a version 9.10.0 1602886.

Artificial neural networks started with McCulloch and Pitts (1943) who developed a computational model for neural networks based on algorithms called threshold logic. This model paved the way for the division of the research into two ways. One strategy concentrated on biological processes, while the other concentrated on using neural networks to create artificial intelligence. Artificial neural networks were driven to address the various facets or components of learning, such as how to learn, how to induce, and how to deduce, just like other artificial intelligence algorithms. For instance, ANN can serve a predictive tool for drug design, discovery, delivery, and disposition (Puri et al., 2016). Also, ANN is regarded as an effective and potent instrument for tackling complicated engineering and scientific problems (Shao et al., 2019), but some of its flaws include the lengthy training period, a large number of parameters, and undesirable convergence (Inthachot et al., 2016; Momeni et al., 2014). The simplicity and naturalness of an ANN model allow it to handle extremely complicated real-world issues in a nonparallel and distributive manner, much like a biological neural network (Puri et al., 2016). Fig. 1 illustrates an ANN network structure, while Eq. (3) explains how ANN is mathematically described.

$$Y(t) = F\left(\sum_{i=1}^{n}(Xi(t)Wi(t) + c)\right) \quad (3)$$

where Xi(t) is the input value at time t, Wi(t) is the weight of neural input at time t, c is the bias, F is a transfer function, Y(t) is the output value at time t.

The input, hidden, and output layers are the three primary components of an ANN's structure (Ababneh et al., 2020; Ahmad et al., 2018; Haddad and Haddad, 2021; Mohtasham Moein et al., 2023). The input layer stores input parameters and transmits them for model training and testing. The hidden layer (middle) is crucial to the architecture of ANNs and is responsible for the link between the input layer and the output layer. Each hidden layer contains a collection of neurons. The output layer is a layer in charge of creating the outcome. In this procedure, the network receives training data during the training phase, and the network weights are changed to reduce the error between the current output and the target or to reach a set number of training iterations. A crucial step in modeling neural networks is choosing the number of neurons and hidden layers; if there are no enough hidden layers, the model will not have the learning resources to handle complicated and nonlinear issues. On the other side, a big number of hidden layers and neurons will lengthen training time. By learning behaviors other than the link between the parameters in the network, the model may perform badly in addressing issues (Asteris and Mokos, 2020; Chithra et al., 2016a; Xu et al., 2019).

In order to fit multi-dimensional mapping issues arbitrarily well, provide consistent data, and have enough neurons in its hidden layer, a two-layer feed-forward network with sigmoid hidden neurons and linear output neurons was used in this study (Mohtasham Moein et al., 2023). Scaled conjugate gradient, Levenberg-Marquardt, and Bayesian regularization backpropagations were used to train the network, teach data, and finally report satisfactory results of training algorithms use. The sigmoid activation operation applies the sigmoid function to set all values in the input data to a value between 0 and 1. This operation is

Table 1
Data statistics.

Variable	Mean	StDev	Minimum	Median	Maximum	Skewness	Kurtosis
^{226}Ra	251.9	524.4	0.0	118.0	6428.0	8.77	97.61
^{232}Th	145.0	333.3	0.0	63.0	4000.0	8.40	90.46
^{40}K	760	3566	0	240	36000	9.62	93.67
H_{in}	2.079	3.370	0.010	1.190	36.400	6.53	58.00
H_{ex}	1.399	2.172	0.010	0.810	19.000	5.42	38.12

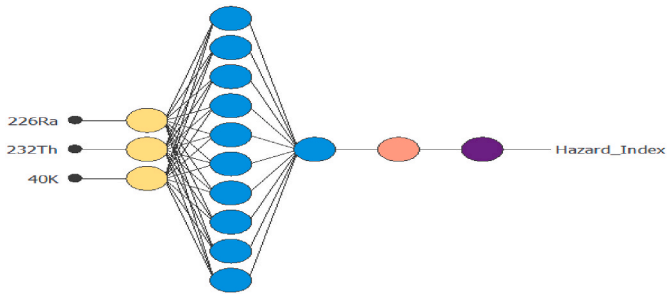

Fig. 2. Neural network architecture.

illustrated in Eq. (4):

$$f(x) = \frac{1}{1 + e^{-x}} \tag{4}$$

A total of three input variables comprising ^{226}Ra, ^{232}Th, and ^{40}K and a single target variable, hazard index were added to create the neural network. Out of 203 samples surveyed for the study, 70% was utilized as training samples, 15% as validation samples, and 15% as testing samples. Training repeatedly results in a variety of results due to the different beginning conditions and sampling. Consequently, the randomness, overfitting, and under fitting were, however, prevented by implementing a function and providing the ANN with a random stream to achieve higher model performance by generalizing an independent dataset. The basic statistics of the data are presented in Table 1. The neural network architecture is displayed in Fig. 2, indicating three input arguments (^{226}Ra, ^{232}Th, and ^{40}K), one hidden layer with 10 neurons, and one output (hazard index).

Two different performance metrics were used in this study: the correlation coefficient (R) and the mean square error (MSE). The higher the value of R to 1, the stronger the prediction. However, the lower the MSE to 0, the better the prediction (Cort J. Willmott and Kenji Matsuura, 2005). The performance metrics are expressed in Eqs. (5) and (6):

$$R = 1 - \frac{\sum_{i=1}^{n}\left(y_i^{pred} - y_i^{actual}\right)}{\sum_{i=1}^{n}\left(y_i^{pred} - \overline{y_i^{actual}}\right)} \tag{5}$$

$$MSE = \frac{1}{n}\sum_{i=1}^{n}\left(y_i^{pred} - y_i^{actual}\right)^2 \tag{6}$$

5. Results and discussion

5.1. Industrial byproducts

Table 2 (a)-(g) describe the radiological characteristics of the investigated industrial byproducts. As shown in Table 1 (a)–(g), some industrial byproducts were higher than the UNSCEAR-set global population-weighted averages (United Nations Scientific Committee on the Effects of Atomic Radiation, 2008, 2000) for activity concentrations and hazard indexes. For instance, the world population-weighted average indoor hazard in bottom ash (BA) was 30% above unity because its ^{226}Ra concentration (196 Bq kg^{-1}) exceeded the upper limit of 185 Bq kg^{-1}. However, its ^{226}Ra concentration, which radon exhalation produces to cause an outdoor concentration of 196 Bq kg^{-1}, was less than the upper limit 370 Bq kg^{-1}, hence, its outdoor hazard was 10% lower than the acceptable amount (NORDIC, 2000; Ravisankar et al., 2014; United Nations Scientific Committee on the Effects of Atomic Radiation, 2008; 2000). Similar cases were observed for fly ash (FA), ground granulated blast furnace slag (GGBFS), granite waste powder (GWP), lead slag (LS), and pumice (PM) with approximately 50%, 10%, 29%, 39%, and 4% of indoor hazard values above 1. However, their outdoor hazard values were about 1%, 28%, 1%, 9%, and 35% lower than unity.

Copper slag (CS), biomass ash (BM), mill tailings (MT), phosphogypsum (PG), red mud (RM), tin slag (TS), and volcanic ash (VA) exhibited radiological concerns because their activity concentrations and hazard indexes were higher than the world population-weighted averages. The indoor hazards from CS, BM, MT, PG, RM, TS, and VA were approximately 80%, 75%, 85%, 55%, 71%, 96%, and 47% higher than the world population-weighted averages (United Nations Scientific Committee on the Effects of Atomic Radiation, 2008, 2000). Additionally, their outdoor hazard indexes were 80%, 50%, 71%, 15%, 62%, 93%, and 32% above the world population-weighted averages of UNSCEAR.

Except with ^{226}Ra and ^{232}Th of incinerated sewage sludge ash (ISSA), there are positive results in Table 2 (a)-(g) listing that the activity concentrations of incinerated sewage sludge ash (ISSA), metakaolin (MK), marble powder (MP), nickel slag (NS), pyrite ash (PA), silica fume (SF), steel slag (SS), and waste glass powder (WP) were lower than the upper limit of 185/370 Bq kg^{-1}, 259 Bq kg^{-1}, 4810 Bq kg^{-1} stated for ^{226}Ra, ^{232}Th, and ^{40}K, respectively (United Nations Scientific Committee on the Effects of Atomic Radiation, 2008, 2000). As a result, their hazard indexes were lower than the world population-weighted averages reported by UNSCEAR (United Nations Scientific Committee on the Effects of Atomic Radiation, 2008, 2000). Regarding indoor hazard indexes, ISSA, MK, MP, NS, PA, SF, SS, and WP were around 30%, 2%, 98%, 8%, 89%, 89%, 66%, and 89% lower than the maximum limit of 1. Also, the outdoor hazard indexes from ISSA, MK, MP, NS, PA, SF, SS, and WP were about 48%, 28%, 98%, 30%, 92%, 90%, 77%, and 91% below the peak of 1.

The ambiguity of material mechanisms, geological sources, treatment procedures, processing patterns, and manufacturing processes are crucial aspects influencing the radiological properties of industrial byproducts (Beretka and Mathew, 1985; Fidanchevski et al., 2021; Kocsis et al., 2021; Kovler, 2012; Sahoo et al., 2007; Sas et al., 2019; Trevisi et al., 2018). For instance, PG made from phosphate rock contains more ^{226}Ra concentration than gypsum made from carbonate rock since phosphate rocks are often known for having higher natural radioactivity (Kovler, 2012; Righi and Bruzzi, 2006; Trevisi et al., 2018). These findings suggest that those who use BA, BM, CS, FA, GGBFS, GWP, LS, MT, PG, PM, RM, TS, and VA may be exposed to hazard radiation from these byproducts. Only ISSA, MK, MP, NS, PA, SF, SS, and WP met the world population-weighted averages of the studied hazard indexes, based on the maximum allowable limit of 1. Consequently, they are suitable for use as building materials, but only with care.

5.2. Artificial neural networks of machine learning algorithm

Based on the training, validation, and testing of input arguments (^{226}Ra, ^{232}Th, and ^{40}K) and target variable (H_{ex} and H_{in}), as presented in Tables 1 and 2, the indoor and outdoor hazard indexes' performance metrics for the ANN of machine learning technique are shown in Tables 3 and 4. Comparing the Levenberg-Marquardt backpropagation technique to other algorithms, Tables 3 and 4 demonstrate unequivocally that it yielded the best metrics for predicting the indoor and outdoor hazards from industrial byproducts. This could be explained by the fact that it trains moderate-sized feedforward neural networks quickly (up to several hundred weights). It trains neural networks at a rate 10–100 times faster than the usual gradient descent backpropagation (Hagan and Menhaj, 1994; Nawi et al., 2013). Similarly, the results from the Bayesian regularization approach, as shown in Tables 2 and 3, showed comparable performance indicators to the Levenberg-Marquardt backpropagation algorithm but had no correlation coefficient (R) and mean square error (MSE) for validating datasets. Bayesian regularization minimizes the linear combination of squared errors and weights within the Levenberg-Marquardt backpropagation algorithm. As a result, validation terminates at the maximum validation failures to allow further training to find the ideal balance between errors

Table 2
Radiological characteristics of the industrial byproducts analyzed.

(a) Bottom ash (BA), biomass ash (BM), and copper slag (CS)

Material	A (Bq kg^{-1})			H_{ex}	H_{in}	Reference
	^{226}Ra	^{232}Th	^{40}K			
BA	306	65	233	1.13	1.95	Sas et al. (2019)
BA	113	68	623	0.70	1.00	Sas et al. (2019)
BA	345	59	410	1.25	2.18	Trevisi et al. (2018)
BA	423	35	296	1.34	2.48	Petropoulos et al. (2002)
BA	139	108	292	0.85	1.23	Amin et al. (2013)
BA	56	63	210	0.44	0.59	(X. Lu et al., 2012)
BA	62	53	457	0.47	0.63	Mishra (2004)
BA	663	44	397	2.04	3.84	Karangelos et al. (2004)
BA	114	124	210	0.83	1.14	Yu (1996)
BA	100	105	132	0.70	0.97	Tso and Leung (1996)
BA	94	105	272	0.72	0.97	(X. Lu et al., 2012)
BA	70	40	355	0.42	0.61	(Puch et al., 2005)
BA	108	79	514	0.70	1.00	Zeller (1995)
BA	541	102	714	2.00	3.47	Schroeyers et al. (2018)
BA	68	74	225	0.52	0.70	Khan et al. (2020)
BA	70	64	457	0.53	0.72	Fidanchevski et al. (2021)
BA	66	97	170	0.59	0.77	Sanjuán et al. (2019)
Average	196	76	351	0.90	1.43	
BM	12	7	36000	7.54	7.58	Alonso et al. (2020)
BM	10	6	6000	1.30	1.32	Alonso et al. (2020)
BM	9	4	35898	7.50	7.53	Puertas et al. (2021)
Average	10	6	25966	5.00	5.00	
CS	1135	50	585	3.38	6.45	Schroeyers et al. (2018)
CS	770	52	650	2.42	4.50	Schroeyers et al. (2018)
CS	317	54	886	1.25	2.11	Schroeyers et al. (2018)
CS	317	54	887	1.25	2.11	(Zak et al., 2008)
CS	770	52	650	2.42	4.50	Lehmann (1996)
Average	662	52	732	2.00	4.00	
Global	33	45	420	≤1	≤1	*(United Nations Scientific Committee on the Effects of Atomic Radiation, 2008, 2000)

(b) Fly ash (FA)

Material	A (Bq kg^{-1})			H_{ex}	H_{in}	Reference
	^{226}Ra	^{232}Th	^{40}K			
FA	119	91	438	0.76	1.09	Sas et al. (2017)
FA	78	126	374	0.78	0.99	Mishra (2004)
FA	904	53	454	2.74	5.19	Karangelos et al. (2004)
FA	100	108	388	0.77	1.04	Alonso et al. (2020)
FA	88	88	868	0.76	1.00	Alonso et al. (2018)
FA	188	91	343	0.93	1.44	Schroeyers et al. (2018)
FA	999	200	1100	3.70	6.40	Schroeyers et al. (2018)
FA	191	91	561	0.98	1.50	Trevisi et al. (2018)
FA	232	117	466	1.18	1.80	Turhan (2009)
FA	825	53	402	2.52	4.75	Petropoulos et al. (2002)
FA	45	40	88	0.29	0.42	Kumar et al. (1999)
FA	126	89	793	0.85	1.19	Gökçe et al. (2020)
FA	14	20	1148	0.35	0.39	Puch et al. (2005)
FA	41	49	321	0.37	0.48	Ademola and Onyema (2014)
FA	99	113	309	0.77	1.04	Mahur et al. (2008)
FA	139	82	743	0.85	1.22	Sas et al. (2019)
FA	83	87	235	0.61	0.83	(X. Lu et al., 2012)
FA	70	79	233	0.54	0.73	(X. Lu et al., 2012)
FA	100	180	650	1.10	1.37	European Commission (1999)
FA	80	207	546	1.13	1.35	Nuccetelli et al. (2015)
FA	90	66	240	0.55	0.79	Ignjatović et al. (2017)
FA	999	56	470	3.01	5.71	Peppas et al. (2010)
FA	161	156	584	1.16	1.59	Peppas et al. (2010)
FA	119	147	352	0.96	1.28	Gupta et al. (2013)
FA	118	157	1463	1.23	1.55	Asaduzzaman et al. (2015)
FA	441	110	510	1.72	2.91	Feng and Lu (2016)
FA	242	31	382	0.85	1.51	Temuujin et al. (2014)
FA	263	49	216	0.94	1.66	Temuujin et al. (2014)
FA	143	117	719	0.99	1.37	Fidanchevski et al. (2021)
FA	75	104	1030	0.82	1.02	Sanjuán et al. (2019)
Average	239	99	548	1.00	2.00	
Global	33	45	420	≤1	≤1	(United Nations Scientific Committee on the Effects of Atomic Radiation, 2008, 2000)

(c) Ground granulated blast furnace slag (GGBFS)

Material	A (Bq kg^{-1})			H_{ex}	H_{in}	Reference
	^{226}Ra	^{232}Th	^{40}K			

(continued on next page)

Table 2 (*continued*)

(c) Ground granulated blast furnace slag (GGBFS)

Material	A (Bq kg^{-1})			H_{ex}	H_{in}	Reference
	^{226}Ra	^{232}Th	^{40}K			
GGBFS	112	52	205	0.55	0.85	Tuo et al. (2020)
GGBFS	182	44	269	0.72	1.21	Sas et al. (2019)
GGBFS	179	55	172	0.73	1.22	Sas et al. (2019)
GGBFS	128	45	119	0.54	0.89	Sas et al. (2019)
GGBFS	89	140	378	0.86	1.10	Mishra (2004)
GGBFS	151	150	14	0.99	1.40	Alonso et al. (2020)
GGBFS	143	163	15	1.02	1.41	Alonso et al. (2020)
GGBFS	98	89	96	0.63	0.89	Alonso et al. (2020)
GGBFS	34	44	846	0.44	0.53	Alonso et al. (2020)
GGBFS	32	35	632	0.35	0.44	Alonso et al. (2020)
GGBFS	97	89	96	0.63	0.89	Alonso et al. (2018)
GGBFS	251	25	362	0.85	1.53	Schroeyers et al. (2018)
GGBFS	323	40	158	1.06	1.93	Schroeyers et al. (2018)
GGBFS	100	100	500	0.76	1.03	Schroeyers et al. (2018)
GGBFS	166	48	232	0.68	1.13	Trevisi et al. (2018)
GGBFS	184	135	283	1.08	1.57	Trevisi et al. (2018)
GGBFS	15	1	20	0.05	0.09	Trevisi et al. (2018)
GGBFS	336	152	786	1.66	2.57	Trevisi et al. (2018)
GGBFS	43	43	76	0.30	0.41	Puertas et al. (2015)
GGBFS	178	148	243	1.10	1.58	Turhan (2009)
GGBFS	67	78	145	0.51	0.69	Kumar et al. (1999)
GGBFS	150	65	142	0.69	1.09	Puch et al. (2005)
GGBFS	35	30	75	0.23	0.32	Puertas et al. (2021)
GGBFS	160	100	250	0.87	1.30	Puertas et al. (2021)
GGBFS	270	70	240	1.05	1.78	European Commission (1999)
GGBFS	251	25	214	0.82	1.50	Sofilić et al. (2010)
GGBFS	117	78	176	0.65	0.97	Mustonen (1984)
GGBFS	115	36	229	0.50	0.81	(Gallyas and Török, 1984)
GGBFS	115	35	192	0.49	0.80	(Zak et al., 2008)
GGBFS	166	48	232	0.68	1.13	Chinchón-Payá et al. (2011)
Average	143	72	247	0.72	1.10	
Global	33	45	420	≤1	≤1	(United Nations Scientific Committee on the Effects of Atomic Radiation, 2008, 2000)

(d) Granite waste powder (GWP), incinerated sewage sludge ash (ISSA), lead slag (LS), and metakaolin (MK)

Material	A (Bq kg^{-1})			H_{ex}	H_{in}	Reference
	^{226}Ra	^{232}Th	^{40}K			
GWP	10	10	299	0.13	0.15	(Harb et al., 2008)
	19	18	956	0.32	0.37	(Harb et al., 2008)
	55	41	398	0.39	0.54	(el Arabi et al., 2007)
	378	154	2285	2.09	3.11	(el Arabi et al., 2007)
	61	48	349	0.42	0.59	(el Arabi et al., 2007)
	886	292	1878	3.91	6.31	(el Arabi et al., 2007)
	71	96	368	0.64	0.83	(el Arabi et al., 2007)
	547	399	1768	3.39	4.86	(el Arabi et al., 2007)
	9	1	2	0.03	0.05	Kobeissi et al. (2013)
	494	157	1776	2.31	3.65	Kobeissi et al. (2013)
	4	15	24	0.07	0.08	Pavlidou et al. (2006)
	91	70	1302	0.79	1.03	Pavlidou et al. (2006)
	2	1	49	0.02	0.02	Krstić et al. (2007)
	170	354	1592	2.16	2.62	Krstić et al. (2007)
	34	46	944	0.47	0.56	Hassan et al. (2010)
	31	45	856	0.44	0.52	Hassan et al. (2010)
	10	29	911	0.33	0.36	Hassan et al. (2010)
	12	37	742	0.33	0.36	Hassan et al. (2010)
	18	64	990	0.50	0.55	Hassan et al. (2010)
Average	153	99	920	0.99	1.40	
ISSA	65	60	563	0.52	0.70	Sas et al. (2019)
Average	65	60	563	0.52	0.70	
LS	270	36	200	0.91	1.64	Croymans et al. (2018)
Average	270	36	200	0.91	1.64	
MK	31	34	188	0.25	0.34	Alonso et al. (2020)
	73	63	136	0.47	0.67	Turhan (2009)
	125	92	695	0.84	1.18	Turhan (2009)
	61	44	590	0.46	0.62	Todorović et al. (2017)
	319	272	1470	2.22	3.08	Todorović et al. (2017)
	18	48	31	0.24	0.29	Adagunodo et al. (2018)
	65	99	157	0.59	0.77	Adagunodo et al. (2018)
	82	98	464	0.70	0.92	Turhan (2009)
Average	97	94	466	0.72	0.98	
Global	33	45	420	≤1	≤1	(United Nations Scientific Committee on the Effects of Atomic Radiation, 2008, 2000)

(*continued on next page*)

Table 2 (*continued*)

(e) Marble powder (MP), mill tailings (MT), nickel slag (NS), pyrite ash (PA), and phosphogypsum (PG)

Material	A (Bq kg^{-1})			H_{ex}	H_{in}	Reference
	^{226}Ra	^{232}Th	^{40}K			

(e) Marble powder (MP), mill tailings (MT), nickel slag (NS), pyrite ash (PA), and phosphogypsum (PG)

Material	A (Bq kg^{-1})			H_{ex}	H_{in}	Reference
	^{226}Ra	^{232}Th	^{40}K			
MP	2	1	10	0.01	0.02	Turhan (2009)
	1	3	25	0.02	0.02	Petropoulos et al. (2002)
	1	4	20	0.02	0.03	Righi and Bruzzi (2006)
	1	1	4	0.01	0.01	Solak et al. (2014)
Average	1	2	15	0.02	0.02	
MT	87	20	226	0.36	0.59	Kamunda et al. (2016)
	2668	89	781	7.72	14.9	Kamunda et al. (2016)
	650	90	740	2.26	4.01	Kocsis et al. (2021)
Average	1135	66	582	3.44	6.51	
NS	52	78	76	0.46	0.60	Schroeyers et al. (2018)
	235	45	605	0.93	1.57	Schroeyers et al. (2018)
Average	143	61	340	0.70	1.08	
PA	3	1	16	0.02	0.02	Turhan (2008)
	23	16	58	0.14	0.20	Turhan (2008)
Average	12	9	37	0.08	0.11	
PG	491	31	68	1.46	2.79	Gezer et al. (2012)
	629	15	10	1.76	3.46	Turhan (2008)
	246	50	340	0.93	1.59	Msila et al. (2016)
	234	21	108	0.74	1.37	Gezer et al. (2012)
	410	182	34	1.82	2.93	Santos et al. (2006)
	209	17	3	0.63	1.20	Trevisi et al. (2012)
	115	31	95	0.45	0.76	Trevisi et al. (2012)
	322	18	116	0.96	1.83	Gezer et al. (2012)
	306	23	17	0.92	1.75	Trevisi et al. (2012)
	305	20	110	0.92	1.75	Trevisi et al. (2012)
	440	12	235	1.28	2.47	Trevisi et al. (2012)
	233	30	323	0.81	1.44	Msila et al. (2016)
	747	14	63	2.09	4.10	Gezer et al. (2012)
	378	4	40	1.05	2.07	Gezer et al. (2012)
	618	9	24	1.71	3.38	Gezer et al. (2012)
	340	4	200	0.98	1.89	Okeji et al. (2012)
	35	72	585	0.49	0.59	Msila et al. (2016)
	750	1	14	2.03	4.06	Roper et al. (2013)
Average	378	31	133	1.17	2.19	
Global	33	45	420	≤1	≤1	(United Nations Scientific Committee on the Effects of Atomic Radiation, 2008, 2000)

(f) Pumice (PM) and red mud/bauxite powder (RM)

Material	A (Bq kg^{-1})			H_{ex}	H_{in}	Reference
	^{226}Ra	^{232}Th	^{40}K			
PM	12	12	300	0.14	0.17	Turhan (2008)
	24	21	653	0.28	0.35	Turhan (2008)
	75	74	1073	0.71	0.91	Trevisi et al. (2018)
	462	57	1	1.47	2.72	Trevisi et al. (2018)
Average	143	41	507	0.65	1.04	
RM	310	1350	350	6.12	6.96	Nuccetelli et al. (2015)
	139	350	45	1.74	2.11	Schroeyers et al. (2018)
	380	507	361	3.06	4.09	Nuccetelli et al. (2015)
	306	408	33	2.41	3.24	Xhixha et al. (2013)
	289	285	121	1.91	2.69	Nuccetelli et al. (2015)
	97	118	15	0.72	0.98	Schroeyers et al. (2018)
	710	339	300	3.29	5.21	Schroeyers et al. (2018)
	210	539	112	2.67	3.24	Schroeyers et al. (2018)
	165	328	53	1.72	2.17	Nuccetelli et al. (2015)
	347	283	48	2.04	2.98	Nuccetelli et al. (2015)
	370	328	265	2.32	3.32	Nuccetelli et al. (2015)
	232	344	45	1.96	2.59	Nuccetelli et al. (2015)
	379	472	21	2.85	3.88	Nuccetelli et al. (2015)
	370	437	505	2.79	3.79	Nuccetelli et al. (2015)
	350	414	583	2.67	3.61	Nuccetelli et al. (2015)
	478	555	401	3.52	4.81	Nuccetelli et al. (2015)
	255	422	164	2.35	3.04	Nuccetelli et al. (2015)
	477	705	153	4.04	5.33	Nuccetelli et al. (2015)
	326	1129	30	5.25	6.13	Nuccetelli et al. (2015)
	318	1320	190	6.00	6.85	("Radiological Assessment for Bauxite Mining and Alumina Refining," 2012)
	17	63	625	0.42	0.47	Tuo et al. (2020)
	100	113	55	0.72	0.99	Alonso et al. (2020)
	97	118	50	0.73	0.99	Trevisi et al. (2018)

(*continued on next page*)

Table 2 (*continued*)

(f) Pumice (PM) and red mud/bauxite powder (RM)						
Material	A (Bq kg^{-1})			H_{ex}	H_{in}	Reference
	^{226}Ra	^{232}Th	^{40}K			
	301	539	215	2.94	3.75	Trevisi et al. (2018)
	170	404	26	2.02	2.48	Puertas et al. (2021)
	203	598	62	2.87	3.42	Rubinos and Barral (2013)
	225	219	5	1.45	2.06	Somlai et al. (2008)
	568	392	101	3.07	4.60	Somlai et al. (2008)
Average	292	467	176	2.63	3.42	
Global	33	45	420	≤1	≤1	(United Nations Scientific Committee on the Effects of Atomic Radiation, 2008, 2000)
(g) Silica fume (SF), steel slag (SS), tin slag (TS), volcanic ash (VA), And waste glass powder (WP)						
Material	A (Bq kg-1)			H_{ex}	H_{in}	Reference
	^{226}Ra	^{232}Th	^{40}K			
SF	2	3	100	0.04	0.04	Puertas et al. (2015)
	1	2	92	0.03	0.03	Puertas et al. (2015)
	1	0	870	0.18	0.19	Gökçe et al. (2020)
	33	24	540	0.29	0.38	Sahoo et al. (2007)
	4	6	297	0.10	0.11	Singovszka et al. (2017)
	0	0	100	0.02	0.02	Alonso et al. (2020)
	0	0	92	0.02	0.02	Alonso et al. (2020)
Average	6	5	299	0.10	0.11	
SS	5	0	1	0.01	0.03	Puch et al. (2005)
	23	21	0	0.14	0.21	Alonso et al. (2020)
	23	15	4	0.12	0.18	Alonso et al. (2020)
	16	20	0	0.12	0.16	Alonso et al. (2020)
	20	16	0	0.12	0.17	Alonso et al. (2020)
	62	21	51	0.26	0.43	Schroeyers et al. (2018)
	23	15	51	0.13	0.19	Schroeyers et al. (2018)
	13	7	21	0.07	0.10	Schroeyers et al. (2018)
	25	5	10	0.09	0.16	Schroeyers et al. (2018)
	196	30	148	0.68	1.21	Schroeyers et al. (2018)
	0	150	0	0.58	0.58	Schroeyers et al. (2018)
	88	49	0	0.43	0.66	Schroeyers et al. (2018)
Average	41	29	24	0.23	0.34	
TS	1100	300	330	4.20	7.20	Schroeyers et al. (2018)
	6428	420	0	19.0	36.4	Schroeyers et al. (2018)
	1000	4000	0	18.1	20.8	Schroeyers et al. (2018)
Average	2843	1573	110	13.8	21.5	
VA	59	132	1130	0.90	1.06	Turhan (2008)
	92	138	1200	1.03	1.28	Righi and Bruzzi (2006)
	190	210	1900	1.72	2.23	Righi and Bruzzi (2006)
	280	270	1900	2.19	2.95	Righi and Bruzzi (2006)
Average	155	188	1533	1.46	1.88	
WP	8	11	227	0.11	0.13	Puertas et al. (2015)
	9	11	2	0.07	0.09	Alonso et al. (2020)
Average	9	11	115	0.09	0.11	
Global	33	45	420	≤1	≤1	(United Nations Scientific Committee on the Effects of Atomic Radiation, 2008, 2000)

*UNSCEAR: United Nations Scientific Committee on the Effects of Atomic Radiation (World Population-Weighted Average Value).

Table 3
ANN's performance metrics for indoor hazard index from industrial byproducts.

Backpropagation algorithm	Network structure	Results	MSE	R
Levenberg-Marquardt	3-10-1-1	Training	0.0000138897	0.999999
	3-10-1-1	Validation	0.0003157730	0.999971
	3-10-1-1	Testing	0.0054188200	0.999430
Bayesian regularization	3-10-1-1	Training	0.0000095357	0.999999
	3-10-1-1	Validation	0.0000000000	0.000000
	3-10-1-1	Testing	0.0003296140	0.999998
Scaled conjugate gradient	3-10-1-1	Training	0.1039780000	0.996285
	3-10-1-1	Validation	0.0639470000	0.982601
	3-10-1-1	Testing	0.9061260000	0.952582

Table 4
ANN's performance metrics for outdoor hazard index from industrial byproducts.

Backpropagation algorithm	Network structure	Results	MSE	R
Levenberg-Marquardt	3-10-1-1	Training	0.0000066829	0.999999
	3-10-1-1	Validation	0.0000169388	0.999997
	3-10-1-1	Testing	0.0000070187	0.999990
Bayesian regularization	3-10-1-1	Training	0.0000071951	0.999999
	3-10-1-1	Validation	0.0000000000	0.000000
	3-10-1-1	Testing	0.0000066423	0.999997
Scaled conjugate gradient	3-10-1-1	Training	0.0123632000	0.998997
	3-10-1-1	Validation	0.0027506000	0.991540
	3-10-1-1	Testing	0.0038999800	0.999308

and weights (Dan Foresee and Hagan, n.d.; MacKay, 1992).

Willmott and Matsuura (2005) argued that error scales cause the difference in values, and MSE is a useful generalization of the size of mistake. According to this, the effectiveness of how different models handle errors is compared and evaluated using MSE. As a result, Table 4's findings showed that the performance indicators of Levenberg-Marquardt backpropagation algorithm were 99.96%, 99.51%, and 99.40% more error-free for training, validating, and testing datasets than scaled conjugate gradient approach.

Table 5
A summary of studies based on ANN (70% training, 15% validation, and 15% testing).

Backpropagation algorithm	Network structure	Results	MSE	R	Reference
Levenberg-Marquardt	3-10-1-1	Training	0.000157417	0.99999	
	3-10-1-1	Validation	0.000206717	0.99999	Kannaiyan et al. (2020)
	3-10-1-1	Testing	0.000295692	0.99999	
Levenberg-Marquardt		Training	0.00069	0.99152	Gupta et al. (2019)
		Testing	0.00129	0.98826	
		Training	0.00057	0.99307	
		Testing	0.00082	0.99283	
		Training	0.00064	0.99364	
		Testing	0.00057	0.99544	
		Training	0.00062	0.99269	
		Testing	0.00086	0.99197	
		Training	0.00137	0.99149	
		Testing	0.00108	0.99338	
Levenberg-Marquardt		Training	1.572	0.999	Atici (2011)
		Validation	1.920	0.973	
		Testing	1.189	0.990	
Levenberg-Marquardt	4-10-1-1	Training	–	0.9987	Chithra et al. (2016b)
	4-10-1-1	Validation	–	0.9968	
	4-10-1-1	Testing	–	0.9979	
	6-10-1-1	Training	–	0.9988	
	6-10-1-1	Validation	–	0.9986	
	6-10-1-1	Testing	–	0.9991	

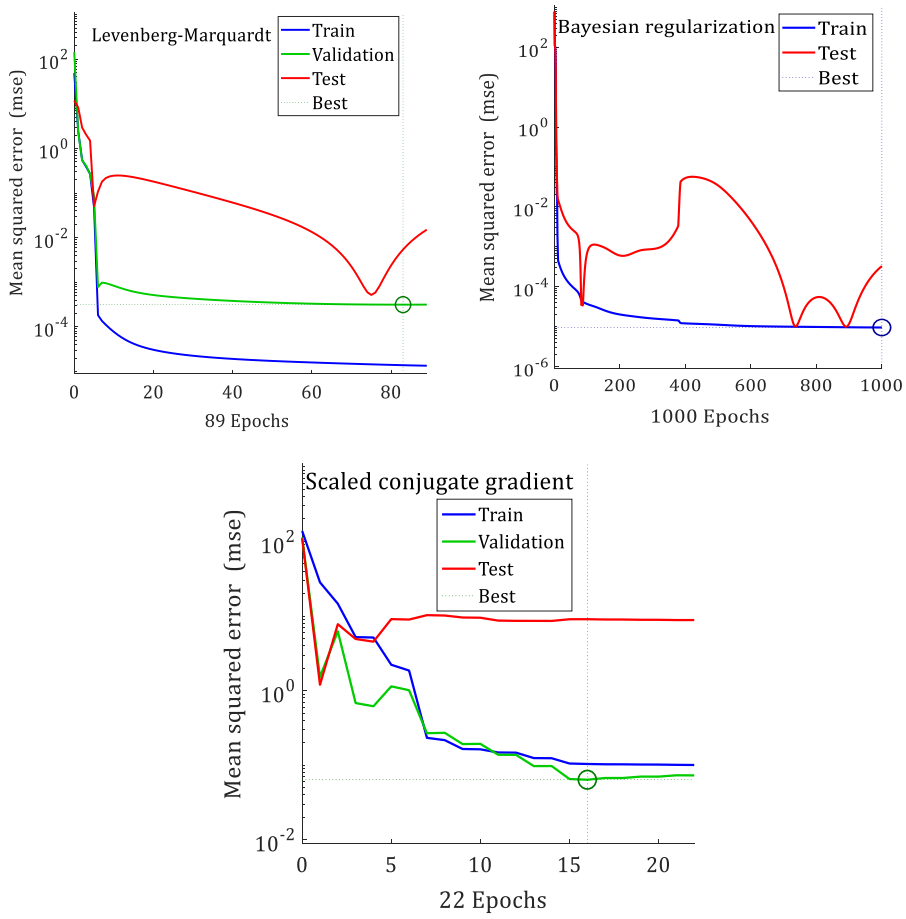

Fig. 3. Best validation performance plots for indoor hazard index.

Table 4 shows that for training and testing the datasets used in forecasting the outdoor hazards from industrial byproducts, the Levenberg-Marquardt backpropagation and Bayesian regularization backpropagation algorithms produced comparable performance metrics (R and MSE). However, when compared to scaled conjugate gradient technique, the Levenberg-Marquardt backpropagation was more precise for training, validating, and testing the anticipated outputs. As was previously indicated, the greater a model's R to unity value, the better it

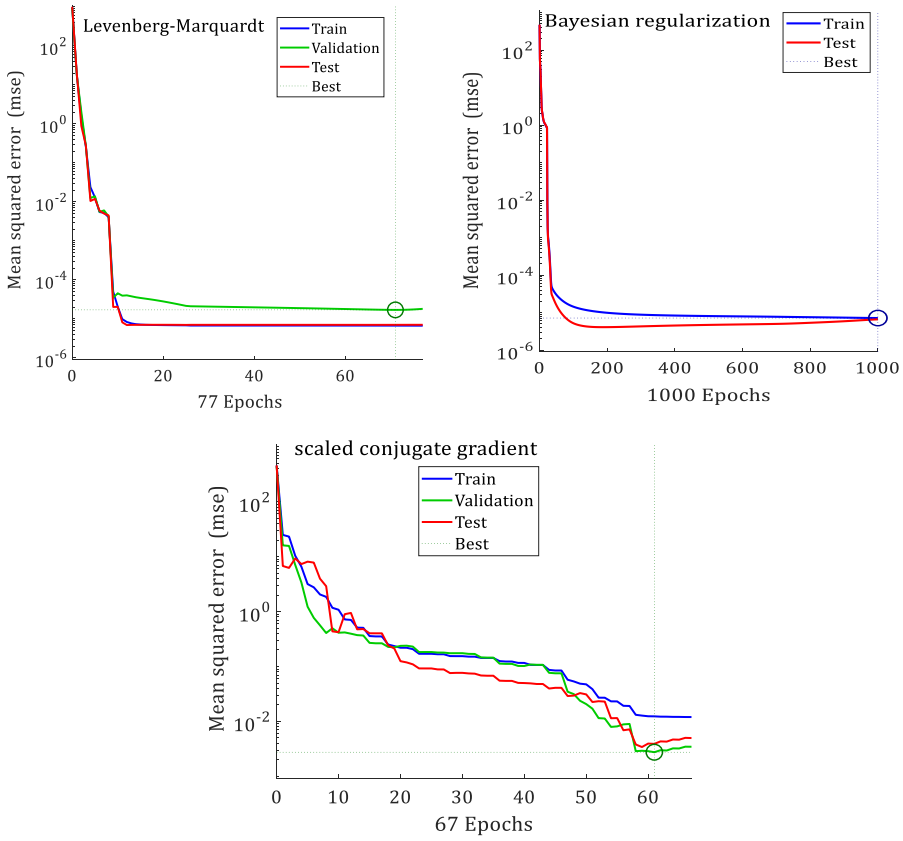

Fig. 4. Best validation performance plots for outdoor hazard index.

can forecast datasets. The performance of the model improves when MSE gets closer to zero. As a result, optimal performance was shown by the performance metrics of ANN for the prediction of indoor and outdoor hazards from industrial byproducts shown in Tables 3 and 4 After analyzing the literature, no information was found on the connection between activity concentrations and hazard indexes of industrial byproducts using machine learning techniques. Tables 3 and 4's results from the Levenberg-Marquardt backpropagation algorithm, however, concur with relevant literature shown in Table 5.

5.3. Mean squared error (MSE) of performance plot

The best training results for the backpropagation training algorithms for the indoor and outdoor hazard indexes are displayed in Figs. 3 and 4, respectively, to show the training performance and error characteristics. In Fig. 3, it is clear that the Levenberg-Marquardt, Bayesian regularization, and scaled conjugate gradient backpropagation algorithms all achieved accuracy of 0.0031577, 0.0000095357, and 0.063947 at epochs 83, 1000, and 16, respectively, validating results presented in Table 2. Similarly, the best validation performance for Levenberg-Marquardt, Bayesian regularization, and scaled conjugate gradient backpropagation algorithms, as shown in Fig. 4, attained accuracy of 0.000016939, 0.0000071951, and 0.0027506 at epochs 71, 1000, and 61, respectively. These findings support the results highlighted in Table 3. Figs. 3 and 4 show that the data match the model well due to good training, and it is therefore concluded that a network system with better training produces results with the least amount of error and can also be used to forecast future values that are unknown at the moment.

5.4. Regression plots of training, testing, and validation

Fig. 5 shows the correlation coefficients for training, validation, testing and combined set for indoor hazard index. As indicated in Fig. 5, the combined set of all yielded 99.997%, 100%, and 95.232% R-values for Levenberg-Marquardt, Bayesian regularization, and scaled conjugate gradient backpropagation algorithms of ANN, respectively. Better correlation was reported in Fig. 6 for outdoor hazard index, where combined set of all generated 100%, 100%, and 99.902% R-values for Levenberg-Marquardt, Bayesian regularization, and scaled conjugate gradient backpropagation algorithms of ANN, respectively. These indicate that the selected network structure (3–10–1–1) has no error. The correlation between the output and the desired (target) value is indicated by the regression coefficient value. When the R-value is 100%, the output and the target have a very close relationship. According to relevant studies, if R-value is 0, there is a random relationship; if R-value is larger than 90%, the result is of better quality (Dao et al., 2019; Gupta et al., 2019; Kannaiyan et al., 2020; Shahmansouri et al., 2021; Vettivel et al., 2013).

6. Conclusions

Artificial neural network's prediction of the indoor and outdoor hazards from industrial byproducts was carried out. The model was developed based on the data obtained from the naturally occurring radioactive materials and relevant studies and it was trained and tested. In addition, the backpropagation model networks were developed and the accuracy of the trained network was accessed by comparing the predicted value against the data value. The indoor and outdoor hazard indexes of ANN modelling techniques were examined and compared in this study. Based on the comparison and study the following conclusions are drawn:

a. With the exception of ISSA, MK, MP, NS, PA, SF, SS, and WP, all surveyed industrial byproducts pose indoor and outdoor hazards.

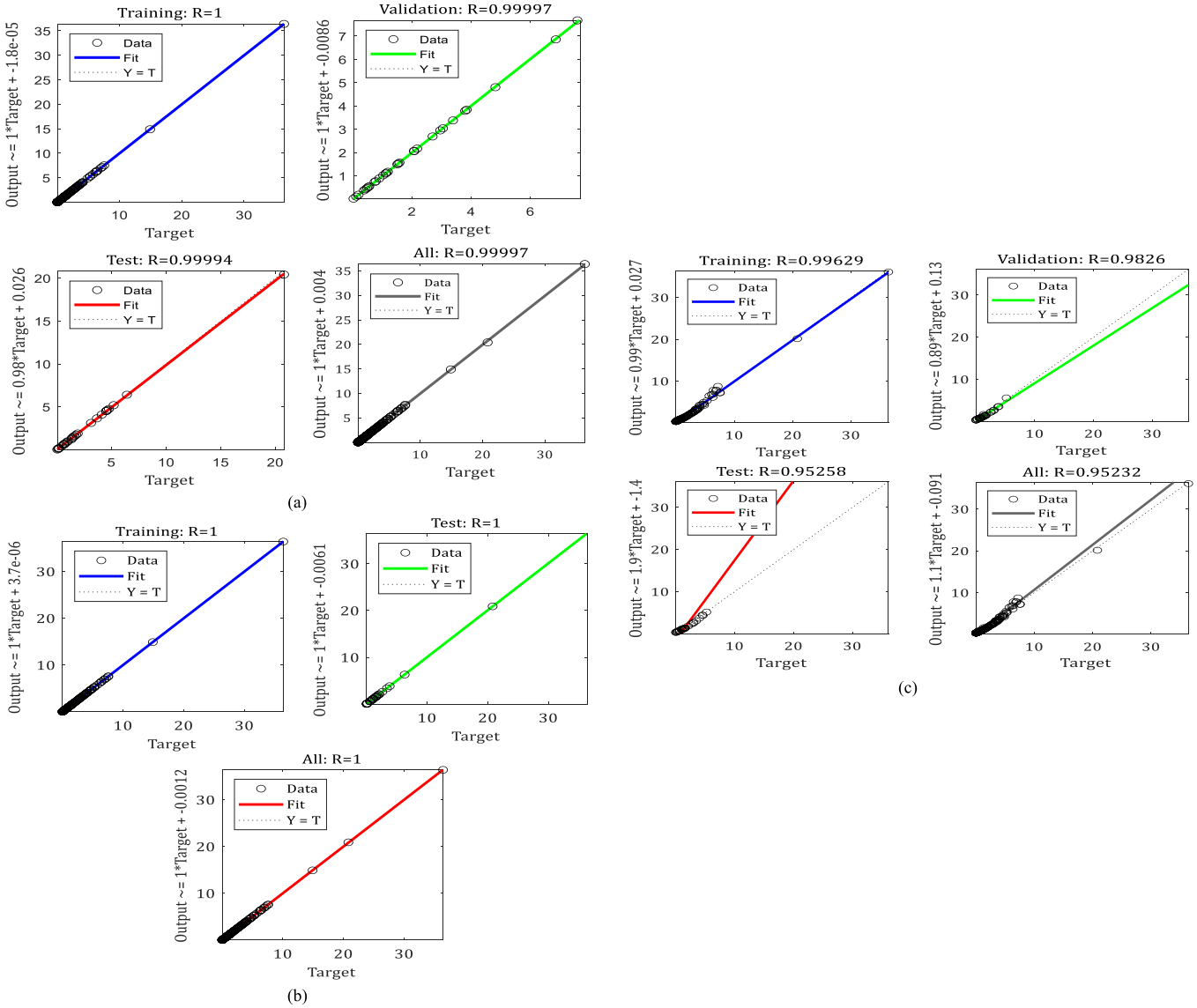

Fig. 5. Indoor hazard regression plots for (a) Levenberg-Marquardt, (b) Bayesian regularization, and (c) scaled conjugate gradient backpropagation algorithms of ANN.

b. The indoor and outdoor hazards from ISSA, MK, MP, NS, PA, SF, SS, and WP were about 2–98% lower than the world population-weighted average value of UNSCEAR.
c. All training, validation, testing, and combined sets, with the exception of the scaled conjugate gradient backpropagation technique for indoor hazards, displayed R-values above 99%, indicating that the chosen network structure (3-10-1-1) is error-free.
d. The backpropagation algorithm network 3–10–1–1 yielded closure outputs with desired (target) values for indoor and outdoor hazards from industrial byproducts.
e. Levenberg-Marquardt and Bayesian regularization backpropagation techniques showed the best performance metrics for training, validating, and testing datasets of hazard indexes from industrial byproducts, according to a comparison of backpropagation model networks.

There is currently little to no study that predicts the indoor and outdoor hazards from industrial byproducts using machine learning techniques. This study filled this knowledge gap and showed that artificial neural network of machine learning algorithms could forecast the indoor and outdoor hazards from industrial byproducts based on the activity concentrations of the ^{226}Ra and ^{232}Th series, as well as the ^{40}K isotopes. Additionally, this study pinpointed certain industrial byproducts that provided indoor and outdoor hazard threats, enlightening potential users about these risks. Despite these promising findings, more research is required to assess the applicability of hazard indexes of industrial byproducts. This research should also include data on the internal and external hazard indexes of other industrial byproducts.

Funding

This research did not receive any specific grant from funding agencies in the public, commercial, or not-for-profit sectors.

Statement of code availability

The statement of code availability is available at https://github.com/Sotech281/Data-trained.

Declaration of competing interest

The authors show a credit to the sources in the manuscript. The

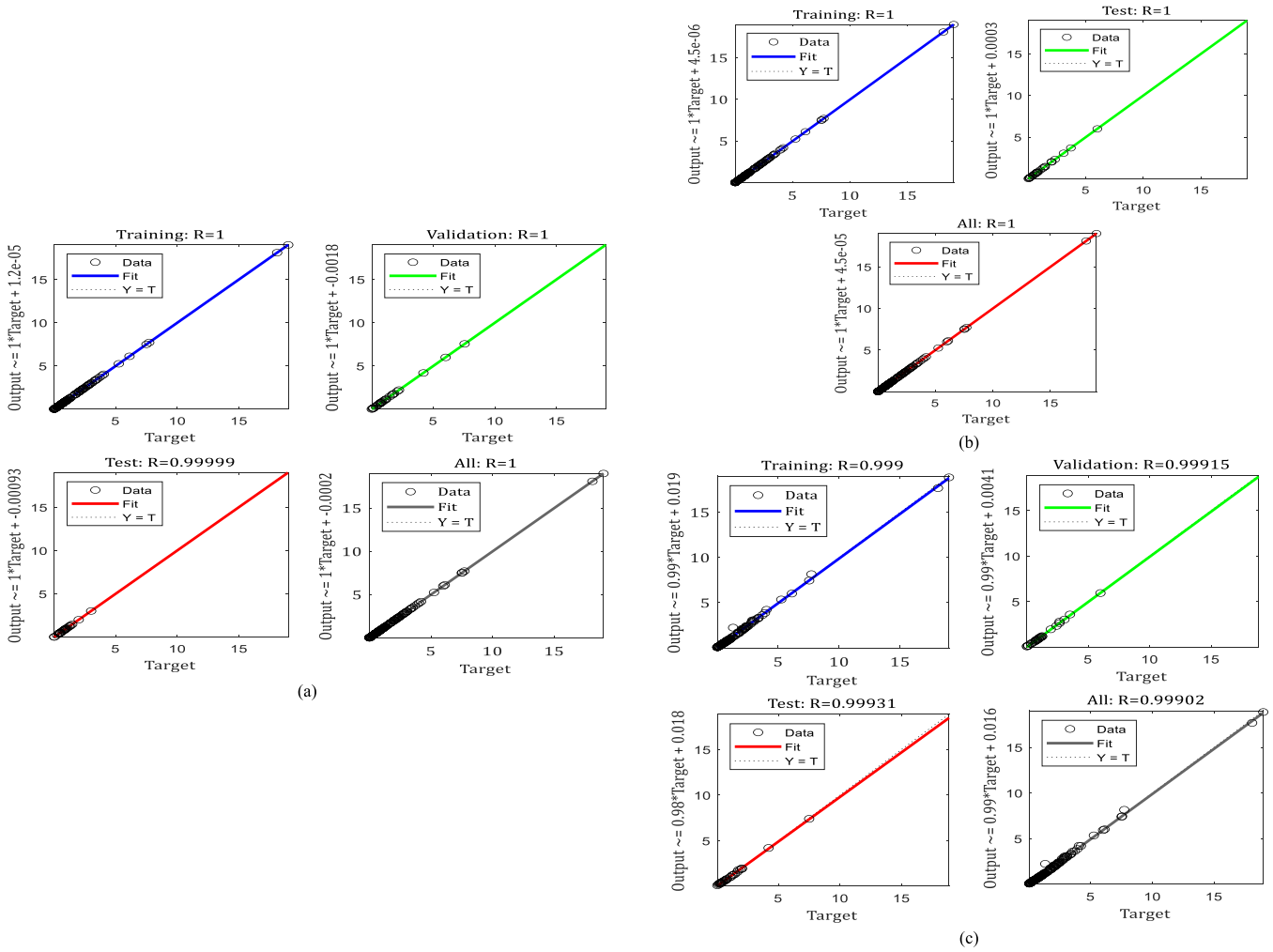

Fig. 6. Outdoor hazard regression plots for (a) Levenberg-Marquardt, (b) Bayesian regularization, and (c) scaled conjugate gradient backpropagation algorithms of ANN.

authors declare that they have no known competing for financial interests or personal relationships that could have appeared to influence the work reported in this paper. The raw/processed data required to reproduce these findings cannot be shared at this time as the Data also forms part of an ongoing study. The authors declare that the manuscript is the authors' original work and has not been published before. The authors also declare that the article contains no libelous or unlawful statements and does not infringe on the rights of others.

Data availability

All data used are indluded and described in the manuscript

Acknowledgement

This work was supported by the Covenant University Centre for Research, Innovation, and Discoveries.

References

Ababneh, A., Alhassan, M., Abu-Haifa, M., 2020. Predicting the contribution of recycled aggregate concrete to the shear capacity of beams without transverse reinforcement using artificial neural networks. Case Stud. Constr. Mater. 13, e00414 https://doi.org/10.1016/j.cscm.2020.e00414.

Abdeljaber, O., Avci, O., Inman, D.J., 2016. Active vibration control of flexible cantilever plates using piezoelectric materials and artificial neural networks. J. Sound Vib. 363, 33–53. https://doi.org/10.1016/j.jsv.2015.10.029.

Adagunodo, T.A., George, A.I., Ojoawo, I.A., Ojesanmi, K., Ravisankar, R., 2018. Radioactivity and radiological hazards from a kaolin mining field in Ifonyintedo, Nigeria. MethodsX 5, 362–374. https://doi.org/10.1016/j.mex.2018.04.009.

Ademola, J.A., Onyema, U.C., 2014. Assessment of natural radionuclides in fly ash produced at orji river thermal power station, Nigeria and the associated radiological impact. Nat. Sci. 6, 752–759. https://doi.org/10.4236/ns.2014.610075.

Ahmad, A., Kotsovou, G., Cotsovos, D.M., Lagaros, N.D., 2018. Assessing the accuracy of RC design code predictions through the use of artificial neural networks. International Journal of Advanced Structural Engineering 10, 349–365. https://doi.org/10.1007/s40091-018-0202-4.

Alonso, M.M., Pasko, A., Gascó, C., Suarez, J.A., Kovalchuk, O., Krivenko, P., Puertas, F., 2018. Radioactivity and Pb and Ni immobilization in SCM-bearing alkali-activated matrices. Construct. Build. Mater. 159, 745–754. https://doi.org/10.1016/j.conbuildmat.2017.11.119.

Alonso, M.M., Suárez-Navarro, J.A., Pérez-Sanz, R., Gascó, C., Moreno de los Reyes, A. M., Lanzón, M., Blanco-Varela, M.T., Puertas, F., 2020. Data on natural radionuclide's activity concentration of cement-based materials. Data Brief 33, 106488. https://doi.org/10.1016/j.dib.2020.106488.

Amin, Y.M., Uddin Khandaker, M., Shyen, A.K.S., Mahat, R.H., Nor, R.M., Bradley, D.A., 2013. Radionuclide emissions from a coal-fired power plant. Appl. Radiat. Isot. 80, 109–116. https://doi.org/10.1016/j.apradiso.2013.06.014.

Aprianti, E., Shafigh, P., Bahri, S., Farahani, J.N., 2015. Supplementary cementitious materials origin from agricultural wastes – a review. Construct. Build. Mater. 74, 176–187. https://doi.org/10.1016/j.conbuildmat.2014.10.010.

Asadi Shamsabadi, E., Roshan, N., Hadigheh, S.A., Nehdi, M.L., Khodabakhshian, A., Ghalehnovi, M., 2022. Machine learning-based compressive strength modelling of concrete incorporating waste marble powder. Construct. Build. Mater. 324, 126592 https://doi.org/10.1016/j.conbuildmat.2022.126592.

Asaduzzaman, K., Mannan, F., Khandaker, M.U., Farook, M.S., Elkezza, A., Amin, Y.B.M., Sharma, S., Abu Kassim, H. bin, 2015. Assessment of natural radioactivity levels and potential radiological risks of common building materials used in Bangladeshi dwellings. PLoS One 10, e0140667. https://doi.org/10.1371/journal.pone.0140667.

Asteris, P.G., Mokos, V.G., 2020. Concrete compressive strength using artificial neural networks. Neural Comput. Appl. 32, 11807–11826. https://doi.org/10.1007/s00521-019-04663-2.

Atici, U., 2011. Prediction of the strength of mineral admixture concrete using multivariable regression analysis and an artificial neural network. Expert Syst. Appl. 38, 9609–9618. https://doi.org/10.1016/j.eswa.2011.01.156.

Avci, O., Abdeljaber, O., Kiranyaz, S., Hussein, M., Gabbouj, M., Inman, D.J., 2021. A review of vibration-based damage detection in civil structures: from traditional methods to Machine Learning and Deep Learning applications. Mech. Syst. Signal Process. 147, 107077 https://doi.org/10.1016/j.ymssp.2020.107077.

Baduge, S.K., Thilakarathna, S., Perera, J.S., Arashpour, M., Sharafi, P., Teodosio, B., Shringi, A., Mendis, P., 2022. Artificial intelligence and smart vision for building and construction 4.0: machine and deep learning methods and applications. Autom. ConStruct. 141, 104440 https://doi.org/10.1016/j.autcon.2022.104440.

Beretka, J., Mathew, P.J., 1985. Natural radioactivity of Australian building materials, industrial wastes and by-products. Health Phys. 48, 87–95. https://doi.org/10.1097/00004032-198501000-00007.

Caridi, F., di Bella, M., Sabatino, G., Belmusto, G., Fede, M.R., Romano, D., Italiano, F., Mottese, A.F., 2021. Assessment of natural radioactivity and radiological risks in river sediments from calabria (southern Italy). Appl. Sci. 11, 1729. https://doi.org/10.3390/app11041729.

Chinchón-Payá, S., Piedecausa, B., Hurtado, S., Sanjuán, M.A., Chinchón, S., 2011. Radiological impact of cement, concrete and admixtures in Spain. Radiat. Meas. 46, 734–735. https://doi.org/10.1016/j.radmeas.2011.06.020.

Chinnu, S.N., Minnu, S.N., Bahurudeen, A., Senthilkumar, R., 2021. Reuse of industrial and agricultural by-products as pozzolan and aggregates in lightweight concrete. Construct. Build. Mater. 302, 124172 https://doi.org/10.1016/j.conbuildmat.2021.124172.

Chithra, S., Kumar, S.R.R.S., Chinnaraju, K., Alfin Ashmita, F., 2016a. A comparative study on the compressive strength prediction models for High Performance Concrete containing nano silica and copper slag using regression analysis and Artificial Neural Networks. Construct. Build. Mater. 114, 528–535. https://doi.org/10.1016/j.conbuildmat.2016.03.214.

Chithra, S., Kumar, S.R.R.S., Chinnaraju, K., Alfin Ashmita, F., 2016b. A comparative study on the compressive strength prediction models for High Performance Concrete containing nano silica and copper slag using regression analysis and Artificial Neural Networks. Construct. Build. Mater. 114, 528–535. https://doi.org/10.1016/j.conbuildmat.2016.03.214.

Council of European Union, 2014. Council Directive 2013/59/Euratom of 5 December 2013 Laying Down Basic Safety Standards for Protection against the Dangers Arising from Exposure to Ionizing Radiation, and Repealing Directives 89/618/Euratom, 90/641/Euratom, 96/29/Euratom, 97/43/Euratom and 2003/122/Euratom. Off. J. Eur. United Nation.

Croymans, T., Leonardi, F., Trevisi, R., Nuccetelli, C., Schreurs, S., Schroeyers, W., 2018. Gamma exposure from building materials – a dose model with expanded gamma lines from naturally occurring radionuclides applicable in non-standard rooms. Construct. Build. Mater. 159, 768–778. https://doi.org/10.1016/j.conbuildmat.2017.10.051.

Dan Foresee, F., Hagan, M.T., n.d. Gauss-Newton approximation to Bayesian learning, in: Proceedings of International Conference on Neural Networks (ICNN'97). IEEE, pp. 1930–1935. https://doi.org/10.1109/ICNN.1997.614194.

Dao, D., Ly, H.-B., Trinh, S., Le, T.-T., Pham, B., 2019. Artificial intelligence approaches for prediction of compressive strength of geopolymer concrete. Materials 12, 983. https://doi.org/10.3390/ma12060983.

Dietterich, T.G., 2000. Ensemble Methods in Machine Learning, pp. 1–15. https://doi.org/10.1007/3-540-45014-9_1.

Dutta, D., Barai, S.v., 2019. Prediction of Compressive Strength of Concrete: Machine Learning Approaches, pp. 503–513. https://doi.org/10.1007/978-981-13-0362-3_40.

el Arabi, A.M., Ahmed, N.K., Salahel Din, K., 2007. Assessment of terrestrial gamma radiation doses for some Egyptian granite samples. Radiat. Protect. Dosim. 128, 382–385. https://doi.org/10.1093/rpd/ncm367.

El-Bahi, S.M., Sroor, A., Mohamed, G.Y., El-Gendy, N.S., 2017. Radiological impact of natural radioactivity in Egyptian phosphate rocks, phosphogypsum and phosphate fertilizers. Appl. Radiat. Isot. 123, 121–127. https://doi.org/10.1016/j.apradiso.2017.02.031.

European Commission, 1999. Radiological Protection Principles Concerning the Natural Radioactivity of Building Materials. Radiation Protection Report -RP-112, Luxembourg.

Feng, T., Lu, X., 2016. Natural radioactivity, radon exhalation rate and radiation dose of fly ash used as building materials in Xiangyang, China. Indoor Built Environ. 25, 626–634. https://doi.org/10.1177/1420326X15573276.

Fidanchevski, E., Angjusheva, B., Jovanov, V., Murtanovski, P., Vladiceska, L., Aluloska, N.S., Nikolic, J.K., Ipavec, A., Šter, K., Mrak, M., Dolenec, S., 2021. Technical and radiological characterisation of fly ash and bottom ash from thermal power plant. J. Radioanal. Nucl. Chem. 330, 685–694. https://doi.org/10.1007/s10967-021-07980-w.

Gallyas, M., Török, I., 1984. Natural radioactivity of raw materials and products in the cement industry. Radiat. Protect. Dosim. 7, 69–71. https://doi.org/10.1093/oxfordjournals.rpd.a082965.

Gaur, V.K., Sharma, P., Sirohi, R., Awasthi, M.K., Dussap, C.-G., Pandey, A., 2020. Assessing the impact of industrial waste on environment and mitigation strategies: a comprehensive review. J. Hazard Mater. 398, 123019 https://doi.org/10.1016/j.jhazmat.2020.123019.

Gezer, F., Turhan, Ş., Uğur, F.A., Gören, E., Kurt, M.Z., Ufuktepe, Y., 2012. Natural radionuclide content of disposed phosphogypsum as TENORM produced from phosphorus fertilizer industry in Turkey. Ann. Nucl. Energy 50, 33–37. https://doi.org/10.1016/j.anucene.2012.07.018.

Ghahramani, Z., 2015. Probabilistic machine learning and artificial intelligence. Nature 521, 452–459. https://doi.org/10.1038/nature14541.

Gökçe, H.S., Canbaz Öztürk, B., Çam, N.F., Andiç-Çakır, Ö., 2020. Natural radioactivity of barite concrete shields containing commonly used supplementary materials. Construct. Build. Mater. 236, 117569 https://doi.org/10.1016/j.conbuildmat.2019.117569.

Gupta, M., Mahur, A.K., Varshney, R., Sonkawade, R.G., Verma, K.D., Prasad, R., 2013. Measurement of natural radioactivity and radon exhalation rate in fly ash samples from a thermal power plant and estimation of radiation doses. Radiat. Meas. 50, 160–165. https://doi.org/10.1016/j.radmeas.2012.03.015.

Gupta, T., Patel, K.A., Siddique, S., Sharma, R.K., Chaudhary, S., 2019. Prediction of mechanical properties of rubberised concrete exposed to elevated temperature using ANN. Measurement 147, 106870. https://doi.org/10.1016/j.measurement.2019.106870.

Haddad, R., Haddad, M., 2021. Predicting fiber-reinforced polymer–concrete bond strength using artificial neural networks: a comparative analysis study. Struct. Concr. 22, 38–49. https://doi.org/10.1002/suco.201900298.

Haenlein, M., Kaplan, A., 2019. A brief history of artificial intelligence: on the past, present, and future of artificial intelligence. Calif. Manag. Rev. 61, 5–14. https://doi.org/10.1177/0008125619864925.

Hagan, M.T., Menhaj, M.B., 1994. Training feedforward networks with the Marquardt algorithm. IEEE Trans. Neural Network. 5, 989–993. https://doi.org/10.1109/72.329697.

Harb, S., E. K, A.H., A.E.M, A.I., A, A., R, W., 2008. Concentration of U-238, U-235, Ra-226, Th-232 and K-40 for some granite samples in eastern desert of Egypt. In: Proc. Third Environ. Phys. Conf., p. 335. Aswan, Egypt.

Hassan, N.M., Ishikawa, T., Hosoda, M., Sorimachi, A., Tokonami, S., Fukushi, M., Sahoo, S.K., 2010. Assessment of the natural radioactivity using two techniques for the measurement of radionuclide concentration in building materials used in Japan. J. Radioanal. Nucl. Chem. 283, 15–21. https://doi.org/10.1007/s10967-009-0050-6.

Ignjatović, I., Sas, Z., Dragaš, J., Somlai, J., Kovács, T., 2017. Radiological and material characterization of high volume fly ash concrete. J. Environ. Radioact. 168, 38–45. https://doi.org/10.1016/j.jenvrad.2016.06.021.

Imani, M., Adelikhah, M., Shahrokhi, A., Azimpour, G., Yadollahi, A., Kocsis, E., Toth-Bodrogi, E., Kovács, T., 2021. Natural radioactivity and radiological risks of common building materials used in Semnan Province dwellings, Iran. Environ. Sci. Pollut. Control Ser. 28, 41492–41503. https://doi.org/10.1007/s11356-021-13469-6.

İnce, O., Yıldız, H., Kisbet, T., Ertürk, Ş.M., Önder, H., 2022. Classification of retinoblastoma-1 gene mutation with machine learning-based models in bladder cancer. Heliyon 8, e09311. https://doi.org/10.1016/j.heliyon.2022.e09311.

Inthachot, M., Boonjing, V., Intakosum, S., 2016. Artificial neural network and genetic algorithm hybrid intelligence for predicting Thai stock price index trend. Comput. Intell. Neurosci. 1–8. https://doi.org/10.1155/2016/3045254, 2016.

Jiang, X., Mahadevan, S., Adeli, H., 2007. Bayesian wavelet packet denoising for structural system identification. Struct. Control Health Monit. 14, 333–356. https://doi.org/10.1002/stc.161.

Joel, E.S., Maxwell, O., Adewoyin, O.O., Olawole, O.C., Arijaje, T.E., Embong, Z., Saeed, M.A., 2019. Investigation of natural environmental radioactivity concentration in soil of coastaline area of Ado-Odo/Ota Nigeria and its radiological implications. Sci. Rep. 9, 4219. https://doi.org/10.1038/s41598-019-40884-0.

Kamunda, C., Mathuthu, M., Madhuku, M., 2016. An assessment of radiological hazards from gold mine tailings in the province of gauteng in South Africa. Int. J. Environ. Res. Publ. Health 13, 138. https://doi.org/10.3390/ijerph13010138.

Kannaiyan, M., karthikeyan, G., Thankachi Raghuvaran, J.G., 2020. Prediction of specific wear rate for LM25/ZrO2 composites using Levenberg–Marquardt backpropagation algorithm. J. Mater. Res. Technol. 9, 530–538. https://doi.org/10.1016/j.jmrt.2019.10.082.

Karangelos, D.J., Petropoulos, N.P., Anagnostakis, M.J., Hinis, E.P., Simopoulos, S.E., 2004. Radiological characteristics and investigation of the radioactive equilibrium in the ashes produced in lignite-fired power plants. J. Environ. Radioact. 77, 233–246. https://doi.org/10.1016/j.jenvrad.2004.03.009.

Kasumović, A., Hankić, E., Kasić, A., Adrović, F., 2018. Natural radioactivity in some building materials and assessment of the associated radiation hazards. Radiochim. Acta 106, 79–86. https://doi.org/10.1515/ract-2017-2809.

Khan, I.U., Sun, W., Lewis, E., 2020. Review of low-level background radioactivity studies conducted from 2000 to date in people Republic of China. J Radiat Res Appl Sci 13, 406–415. https://doi.org/10.1080/16878507.2020.1744330.

Kim, P., 2017. MATLAB Deep Learning. Apress, Berkeley, CA. https://doi.org/10.1007/978-1-4842-2845-6.

Kobeissi, M.A., El-Samad, O., Rachidi, I., 2013. Health assessment of natural radioactivity and radon exhalation rate in granites used as buildingmaterials in Lebanon. Radiat. Protect. Dosim. 153, 342–351. https://doi.org/10.1093/rpd/ncs110.

Kocsis, E., Tóth-Bodrogi, E., Peka, A., Adelikhah, M., Kovács, T., 2021. Radiological impact assessment of different building material additives. J. Radioanal. Nucl. Chem. 330, 1517–1526. https://doi.org/10.1007/s10967-021-07897-4.

Kovler, K., 2012. Radioactive materials. In: Toxicity of Building Materials. Elsevier, pp. 196–240. https://doi.org/10.1533/9780857096357.196.

Krstić, D., Nikezić, D., Stevanović, N., Vučić, D., 2007. Radioactivity of some domestic and imported building materials from South Eastern Europe. Radiat. Meas. 42, 1731–1736. https://doi.org/10.1016/j.radmeas.2007.09.001.

Kumar, V., Ramachandran, T.V., Prasad, R., 1999. Natural radioactivity of Indian building materials and by-products. Appl. Radiat. Isot. 51, 93–96. https://doi.org/10.1016/S0969-8043(98)00154-7.

Kundariya, N., Mohanty, S.S., Varjani, S., Hao Ngo, H., W, C., Wong, J., Taherzadeh, M. J., Chang, J.-S., Yong Ng, H., Kim, S.-H., Bui, X.-T., 2021. A review on integrated approaches for municipal solid waste for environmental and economical relevance: monitoring tools, technologies, and strategic innovations. Bioresour. Technol. 342, 125982 https://doi.org/10.1016/j.biortech.2021.125982.

Langley, P., 2011. The changing science of machine learning. Mach. Learn. 82, 275–279. https://doi.org/10.1007/s10994-011-5242-y.

Legasu, M.L., Chaubey, A.K., 2022. Determination of dose derived from building materials and radiological health related effects from the indoor environment of Dessie city, Wollo, Ethiopia. Heliyon 8, e09066. https://doi.org/10.1016/j.heliyon.2022.e09066.

Lehmann, R., 1996. Strahlenbelastung durch nat€urliche radionuklide in baumaterialien, fossilen brennstoffen und Dungemitteln. Bundesamt fur Strahlenshutz, Berlin.

Ley, C., Bordas, S.P.A., 2018. What makes data science different? A discussion involving Statistics2.0 and computational sciences. Int J Data Sci Anal 6, 167–175. https://doi.org/10.1007/s41060-017-0090-x.

Liu, Q., Sun, P., Fu, X., Zhang, J., Yang, H., Gao, H., Li, Y., 2020. Comparative analysis of BP neural network and RBF neural network in seismic performance evaluation of pier columns. Mech. Syst. Signal Process. 141, 106707 https://doi.org/10.1016/j.ymssp.2020.106707.

Lu, P., Chen, S., Zheng, Y., 2012. Artificial intelligence in civil engineering. Math. Probl Eng. 1–22 https://doi.org/10.1155/2012/145974, 2012.

Lu, X., Li, L.Y., Wang, F., Wang, L., Zhang, X., 2012. Radiological hazards of coal and ash samples collected from Xi'an coal-fired power plants of China. Environ. Earth Sci. 66, 1925–1932. https://doi.org/10.1007/s12665-011-1417-x.

MacKay, D.J.C., 1992. Bayesian interpolation. Neural Comput. 4, 415–447. https://doi.org/10.1162/neco.1992.4.3.415.

Mahur, A.K., Kumar, R., Sengupta, D., Prasad, R., 2008. Estimation of radon exhalation rate, natural radioactivity and radiation doses in fly ash samples from Durgapur thermal power plant, West Bengal, India. J. Environ. Radioact. 99, 1289–1293. https://doi.org/10.1016/j.jenvrad.2008.03.010.

Mandeep, Kumar Gupta, G., Shukla, P., 2020. Insights into the resources generation from pulp and paper industry wastes: challenges, perspectives and innovations. Bioresour. Technol. 297, 122496 https://doi.org/10.1016/j.biortech.2019.122496.

Marani, A., Nehdi, M.L., 2020. Machine learning prediction of compressive strength for phase change materials integrated cementitious composites. Construct. Build. Mater. 265, 120286 https://doi.org/10.1016/j.conbuildmat.2020.120286.

Maxwell, O., Wagiran, H., Ibrahim, N., Lee, S.K., Embong, Z., Ugwuoke, P.E., 2015. Natural radioactivity and geological influence on subsurface layers at Kubwa and Gosa area of Abuja, Northcentral Nigeria. J. Radioanal. Nucl. Chem. 303, 821–830. https://doi.org/10.1007/s10967-014-3442-1.

McCulloch, W.S., Pitts, W., 1943. A logical calculus of the ideas immanent in nervous activity. Bull. Math. Biophys. 5, 115–133. https://doi.org/10.1007/BF02478259.

Mehra, R., Kumar, S., Sonkawade, R., Singh, N.P., Badhan, K., 2010. Analysis of terrestrial naturally occurring radionuclides in soil samples from some areas of Sirsa district of Haryana, India using gamma ray spectrometry. Environ. Earth Sci. 59, 1159–1164. https://doi.org/10.1007/s12665-009-0108-3.

Mishra, U.C., 2004. Environmental impact of coal industry and thermal power plants in India. J. Environ. Radioact. 72, 35–40. https://doi.org/10.1016/S0265-931X(03)00183-8.

Mohtasham Moein, M., Saradar, A., Rahmati, K., Ghasemzadeh Mousavinejad, S.H., Bristow, J., Aramali, V., Karakouzian, M., 2023. Predictive models for concrete properties using machine learning and deep learning approaches: a review. J. Build. Eng. 63, 105444 https://doi.org/10.1016/j.jobe.2022.105444.

Momeni, E., Nazir, R., Jahed Armaghani, D., Maizir, H., 2014. Prediction of pile bearing capacity using a hybrid genetic algorithm-based ANN. Measurement 57, 122–131. https://doi.org/10.1016/j.measurement.2014.08.007.

Mora, J.C., Baeza, A., Robles, B., Sanz, J., 2016. Assessment for the management of NORM wastes in conventional hazardous and nonhazardous waste landfills. J. Hazard Mater. 310, 161–169. https://doi.org/10.1016/j.jhazmat.2016.02.039.

Msila, X., Labuschagne, F., Barnard, W., Billing, D.G., 2016. Radioactive nuclides in phosphogypsum from the lowveld region of South Africa. South Afr. J. Sci. 112, 5. https://doi.org/10.17159/sajs.2016/20150102.

Mustonen, R., 1984. Natural radioactivity in and radon exhalation from Finnish building materials. Health Phys. 46, 1195–1203. https://doi.org/10.1097/00004032-198406000-00003.

Narloch, D.C., Paschuk, S.A., Corrêa, J.N., Rocha, Z., Mazer, W., Torres, C.A.M.P., del Claro, F., Denyak, V., Schelin, H.R., 2019. Characterization of radionuclides present in portland cement, gypsum and phosphogypsum mortars. Radiat. Phys. Chem. 155 https://doi.org/10.1016/j.radphyschem.2018.07.011.

Naseri, H., Jahanbakhsh, H., Hosseini, P., Moghadas Nejad, F., 2020. Designing sustainable concrete mixture by developing a new machine learning technique. J. Clean. Prod. 258, 120578 https://doi.org/10.1016/j.jclepro.2020.120578.

Nawi, N.M., Khan, A., Rehman, M.Z., 2013. A new Levenberg marquardt based back propagation algorithm trained with cuckoo search. Procedia Technology 11, 18–23. https://doi.org/10.1016/j.protcy.2013.12.157.

Nguyen, H., Moayedi, H., Foong, L.K., al Najjar, H.A.H., Jusoh, W.A.W., Rashid, A.S.A., Jamali, J., 2020. Optimizing ANN models with PSO for predicting short building seismic response. Eng. Comput. 36 https://doi.org/10.1007/s00366-019-00733-0.

Nguyen, H., Vu, T., Vo, T.P., Thai, H.-T., 2021. Efficient machine learning models for prediction of concrete strengths. Construct. Build. Mater. 266, 120950 https://doi.org/10.1016/j.conbuildmat.2020.120950.

NORDIC, 2000. Naturally Occurring Radioactivity in the Nordic Countries – Recommendations (Denmark, Finland, Iceland, Norway and Sweden).

Nuccetelli, C., Pontikes, Y., Leonardi, F., Trevisi, R., 2015. New perspectives and issues arising from the introduction of (NORM) residues in building materials: a critical assessment on the radiological behaviour. Construct. Build. Mater. 82, 323–331. https://doi.org/10.1016/j.conbuildmat.2015.01.069.

Okeji, M.C., Agwu, K.K., Idigo, F.U., 2012. Assessment of natural radioactivity in phosphate ore, phosphogypsum and soil samples around a phosphate fertilizer plant in Nigeria. Bull. Environ. Contam. Toxicol. 89, 1078–1081. https://doi.org/10.1007/s00128-012-0811-8.

Olthof, A.W., Shouche, P., Fennema, E.M., Ijpma, F.F.A., Koolstra, R.H.C., Stirler, V.M.A., van Ooijen, P.M.A., Cornelissen, L.J., 2021. Machine learning based natural language processing of radiology reports in orthopaedic trauma. Comput. Methods Progr. Biomed. 208, 106304 https://doi.org/10.1016/j.cmpb.2021.106304.

Oyebisi, S., Ede, A., Olutoge, F., Ngene, B., 2020a. Assessment of activity indexes on the splitting tensile strengthening of geopolymer concrete incorporating supplementary cementitious materials. Mater. Today Commun. 24 https://doi.org/10.1016/j.mtcomm.2020.101356.

Oyebisi, S., Ede, A., Olutoge, F., Omole, D., 2020b. Geopolymer concrete incorporating agro-industrial wastes: effects on mechanical properties, microstructural behaviour and mineralogical phases. Construct. Build. Mater. 256 https://doi.org/10.1016/j.conbuildmat.2020.119390.

Pavlidou, S., Koroneos, A., Papastefanou, C., Christofides, G., Stoulos, S., Vavelides, M., 2006. Natural radioactivity of granites used as building materials. J. Environ. Radioact. 89, 48–60. https://doi.org/10.1016/j.jenvrad.2006.03.005.

Pazouki, G., 2022. Fly ash-based geopolymer concrete's compressive strength estimation by applying artificial intelligence methods. Measurement 203, 111916. https://doi.org/10.1016/j.measurement.2022.111916.

Peppas, T.K., Karfopoulos, K.L., Karangelos, D.J., Rouni, P.K., Anagnostakis, M.J., Simopoulos, S.E., 2010. Radiological and instrumental neutron activation analysis determined characteristics of size-fractionated fly ash. J. Hazard Mater. 181, 255–262. https://doi.org/10.1016/j.jhazmat.2010.05.005.

Petropoulos, N.P., Anagnostakis, M.J., Simopoulos, S.E., 2002. Photon attenuation, natural radioactivity content and radon exhalation rate of building materials. J. Environ. Radioact. 61, 257–269. https://doi.org/10.1016/S0265-931X(01)00132-1.

Puch, K.-H., Bialucha, R., Keller, G., 2005. Naturally Occurring Radioactivity in Industrial By-Products from Coal-Fired Power Plants, from Municipal Waste Incineration and from the Iron- and Steel-Industry, pp. 996–1008. https://doi.org/10.1016/S1569-4860(04)07123-2.

Puertas, F., Alonso, M.M., Torres-Carrasco, M., Rivilla, P., Gasco, C., Yagüe, L., Suárez, J. A., Navarro, N., 2015. Radiological characterization of anhydrous/hydrated cements and geopolymers. Construct. Build. Mater. 101, 1105–1112. https://doi.org/10.1016/j.conbuildmat.2015.10.074.

Puertas, F., Suárez-Navarro, J.A., Alonso, M.M., Gascó, C., 2021. NORM waste, cements, and concretes. A review. Materiales de Construcción 71, e259. https://doi.org/10.3989/mc.2021.13520.

Puri, M., Solanki, A., Padawer, T., Tipparaju, S.M., Moreno, W.A., Pathak, Y., 2016. Introduction to artificial neural network (ANN) as a predictive tool for drug design, discovery, delivery, and disposition. In: Artificial Neural Network for Drug Design, Delivery and Disposition. Elsevier, pp. 3–13. https://doi.org/10.1016/B978-0-12-801559-9.00001-6.

Qamouche, K., Chetaine, A., Elyahyaoui, A., Moussaif, A., Touzani, R., Benkdad, A., Amsil, H., Laraki, K., Marah, H., 2020. Radiological characterization of phosphate rocks, phosphogypsum, phosphoric acid and phosphate fertilizers in Morocco: an assessment of the radiological hazard impact on the environment. Mater. Today Proc. 27, 3234–3242. https://doi.org/10.1016/j.matpr.2020.04.703.

Radiological Assessment for Bauxite Mining and Alumina Refining, 2012. Ann Occup Hyg. https://doi.org/10.1093/annhyg/mes052.

Ravindran, R., Hassan, S., Williams, G., Jaiswal, A., 2018. A review on bioconversion of agro-industrial wastes to industrially important enzymes. Bioengineering 5, 93. https://doi.org/10.3390/bioengineering5040093.

Ravisankar, R., Vanasundari, K., Chandrasekaran, A., Rajalakshmi, A., Suganya, M., Vijayagopal, P., Meenakshisundaram, V., 2012. Measurement of natural radioactivity in building materials of Namakkal, Tamil Nadu, India using gamma-ray spectrometry. Appl. Radiat. Isot. 70, 699–704. https://doi.org/10.1016/j.apradiso.2011.12.001.

Ravisankar, R., Vanasundari, K., Suganya, M., Raghu, Y., Rajalakshmi, A., Chandrasekaran, A., Sivakumar, S., Chandramohan, J., Vijayagopal, P., Venkatraman, B., 2014. Multivariate statistical analysis of radiological data of building materials used in Tiruvannamalai, Tamilnadu, India. Appl. Radiat. Isot. 85, 114–127. https://doi.org/10.1016/j.apradiso.2013.12.005.

Righi, S., Bruzzi, L., 2006. Natural radioactivity and radon exhalation in building materials used in Italian dwellings. J. Environ. Radioact. 88, 158–170. https://doi.org/10.1016/j.jenvrad.2006.01.009.

Roper, A.R., Stabin, M.G., Delapp, R.C., Kosson, D.S., 2013. Analysis of naturally-occurring radionuclides in coal combustion fly ash, gypsum, and scrubber residue samples. Health Phys. 104, 264–269. https://doi.org/10.1097/HP.0b013e318279f3bf.

Rubinos, D.A., Barral, M.T., 2013. Fractionation and mobility of metals in bauxite red mud. Environ. Sci. Pollut. Control Ser. 20, 7787–7802. https://doi.org/10.1007/s11356-013-1477-4.

Sabbarese, C., Ambrosino, F., D'Onofrio, A., Roca, V., 2021. Radiological characterization of natural building materials from the Campania region (Southern Italy). Construct. Build. Mater. 268, 121087 https://doi.org/10.1016/j.conbuildmat.2020.121087.

Sahoo, B.K., Nathwani, D., Eappen, K.P., Ramachandran, T.V., Gaware, J.J., Mayya, Y.S., 2007. Estimation of radon emanation factor in Indian building materials. Radiat. Meas. 42, 1422–1425. https://doi.org/10.1016/j.radmeas.2007.04.002.

Salehi, H., Burgueño, R., 2018. Emerging artificial intelligence methods in structural engineering. Eng. Struct. 171, 170–189. https://doi.org/10.1016/j.engstruct.2018.05.084.

Sanjuán, M.Á., 2022. Coal bottom ash natural radioactivity in building materials. In: Advances in the Toxicity of Construction and Building Materials. Elsevier, pp. 207–224. https://doi.org/10.1016/B978-0-12-824533-0.00006-2.

Sanjuán, M.Á., Quintana, B., Argiz, C., 2019. Coal bottom ash natural radioactivity in building materials. J. Radioanal. Nucl. Chem. 319, 91–99. https://doi.org/10.1007/s10967-018-6251-0.

Santos, A.J.G., Mazzilli, B.P., Fávaro, D.I.T., Silva, P.S.C., 2006. Partitioning of radionuclides and trace elements in phosphogypsum and its source materials based on sequential extraction methods. J. Environ. Radioact. 87, 52–61. https://doi.org/10.1016/j.jenvrad.2005.10.008.

Sas, Z., Doherty, R., Kovacs, T., Soutsos, M., Sha, W., Schroeyers, W., 2017. Radiological evaluation of by-products used in construction and alternative applications; Part I. Preparation of a natural radioactivity database. Construct. Build. Mater. 150, 227–237. https://doi.org/10.1016/j.conbuildmat.2017.05.167.

Sas, Z., Sha, W., Soutsos, M., Doherty, R., Bondar, D., Gijbels, K., Schroeyers, W., 2019. Radiological characterisation of alkali-activated construction materials containing red mud, fly ash and ground granulated blast-furnace slag. Sci. Total Environ. 659, 1496–1504. https://doi.org/10.1016/j.scitotenv.2019.01.006.

Schaubroeck, T., Gibon, T., Igos, E., Benetto, E., 2021. Sustainability assessment of circular economy over time: modelling of finite and variable loops & impact distribution among related products. Resour. Conserv. Recycl. 168, 105319 https://doi.org/10.1016/j.resconrec.2020.105319.

Schroeyers, W., Sas, Z., Bator, G., Trevisi, R., Nuccetelli, C., Leonardi, F., Schreurs, S., Kovacs, T., 2018. The NORM4Building database, a tool for radiological assessment when using by-products in building materials. Construct. Build. Mater. 159, 755–767. https://doi.org/10.1016/j.conbuildmat.2017.11.037.

Shahmansouri, A.A., Yazdani, M., Ghanbari, S., Akbarzadeh Bengar, H., Jafari, A., Farrokh Ghatte, H., 2021. Artificial neural network model to predict the compressive strength of eco-friendly geopolymer concrete incorporating silica fume and natural zeolite. J. Clean. Prod. 279, 123697 https://doi.org/10.1016/j.jclepro.2020.123697.

Shao, Z., Jahed Armaghani, D., Yazdani Bejarbaneh, B., Mu'azu, M.A., Tonnizam Mohamad, E., 2019. Estimating the friction angle of black shale core specimens with hybrid-ANN approaches. Measurement 145, 744–755. https://doi.org/10.1016/j.measurement.2019.06.007.

Sharma, P., Gaur, V.K., Gupta, S., Varjani, S., Pandey, A., Gnansounou, E., You, S., Ngo, H.H., Wong, J.W.C., 2022. Trends in mitigation of industrial waste: global health hazards, environmental implications and waste derived economy for environmental sustainability. Sci. Total Environ. 811, 152357 https://doi.org/10.1016/j.scitotenv.2021.152357.

Shoeib, M.Y., Thabayneh, K.M., 2014. Assessment of natural radiation exposure and radon exhalation rate in various samples of Egyptian building materials. J Radiat Res Appl Sci 7, 174–181. https://doi.org/10.1016/j.jrras.2014.01.004.

Singovszka, E., Estokova, A., Mitterpach, J., 2017. Radioactivity of buildings materials available in Slovakia. IOP Conf. Ser. Earth Environ. Sci. 92, 012054 https://doi.org/10.1088/1755-1315/92/1/012054.

Sofilić, T., Barišić, D., Sofilić, U., 2010. Monitoring of 137Cs in electric arc furnace steel making process. J. Radioanal. Nucl. Chem. 284, 615–622. https://doi.org/10.1007/s10967-010-0513-9.

Solak, S., Turhan, Ş., Uğur, F.A., Gören, E., Gezer, F., Yeğingil, Z., Yeğingil, İ., 2014. Evaluation of potential exposure risks of natural radioactivity levels emitted from building materials used in Adana, Turkey. Indoor Built Environ. 23, 594–602. https://doi.org/10.1177/1420326X12448075.

Somlai, J., Jobbágy, V., Kovács, J., Tarján, S., Kovács, T., 2008. Radiological aspects of the usability of red mud as building material additive. J. Hazard Mater. 150, 541–545. https://doi.org/10.1016/j.jhazmat.2007.05.004.

Stoulos, S., Manolopoulou, M., Papastefanou, C., 2003. Assessment of natural radiation exposure and radon exhalation from building materials in Greece. J. Environ. Radioact. 69, 225–240. https://doi.org/10.1016/S0265-931X(03)00081-X.

Temuujin, J., Minjigmaa, A., Davaabal, B., Bayarzul, U., Ankhtuya, A., Jadambaa, Ts, MacKenzie, K.J.D., 2014. Utilization of radioactive high-calcium Mongolian flyash for the preparation of alkali-activated geopolymers for safe use as construction materials. Ceram. Int. 40, 16475–16483. https://doi.org/10.1016/j.ceramint.2014.07.157.

Todorović, N., Hansman, J., Mrđa, D., Nikolov, J., Kardos, R., Krmar, M., 2017. Concentrations of 226 Ra, 232 Th and 4 0 K in industrial kaolinized granite. J. Environ. Radioact. 168, 10–14. https://doi.org/10.1016/j.jenvrad.2016.07.032.

Trevisi, R., Risica, S., D'Alessandro, M., Paradiso, D., Nuccetelli, C., 2012. Natural radioactivity in building materials in the European Union: a database and an estimate of radiological significance. J. Environ. Radioact. 105, 11–20. https://doi.org/10.1016/j.jenvrad.2011.10.001.

Trevisi, R., Leonardi, F., Risica, S., Nuccetelli, C., 2018. Updated database on natural radioactivity in building materials in Europe. J. Environ. Radioact. 187, 90–105. https://doi.org/10.1016/j.jenvrad.2018.01.024.

Tso, M.W., Leung, J.K.C., 1996. Radiological impact of coal ash from the power plants in Hong Kong. J. Environ. Radioact. 30, 1–14. https://doi.org/10.1016/0265-931X(95)00042-9.

Tuo, F., Peng, X., Zhou, Q., Zhang, J., 2020. Assessment of natural radioactivity levels and radiological hazards in building materials. Radiat. Protect. Dosim. 188, 316–321. https://doi.org/10.1093/rpd/ncz289.

Turhan, Ş., 2008. Assessment of the natural radioactivity and radiological hazards in Turkish cement and its raw materials. J. Environ. Radioact. 99, 404–414. https://doi.org/10.1016/j.jenvrad.2007.11.001.

Turhan, Ş., 2009. Radiological impacts of the usability of clay and kaolin as raw material in manufacturing of structural building materials in Turkey. J. Radiol. Prot. 29, 75–83. https://doi.org/10.1088/0952-4746/29/1/005.

United Nations Scientific Committee on the Effects of Atomic Radiation, 1993. Sources and Effects of Ionizing Radiation, United Nations Scientific Committee on the Effects of Atomic Radiation UNSCEAR 2000 Report to the General Assembly. with Scientific Annexes, New York, NY.

United Nations Scientific Committee on the Effects of Atomic Radiation, 2000. Sources and Effects of Ionizing Radiation, United Nations Scientific Committee on the Effects of Atomic Radiation UNSCEAR 2000 Report to the General Assembly. with Scientific Annexes, New York, NY.

United Nations Scientific Committee on the Effects of Atomic Radiation, 2008. Effects of Ionizing Radiation: Report to the General Assembly. with Scientific Annexes, New York, NY.

United States Environmental Protection Agency, 2008. United States Environmental Protection Agency (Washington, D.C., United States).

United States Environmental Protection Agency, 2022. Technologically Enhanced Naturally Occurring Radioactive Materials (TENORM) (United States).

Vettivel, S.C., Selvakumar, N., Leema, N., 2013. Experimental and prediction of sintered Cu–W composite by using artificial neural networks. Mater. Des. 45, 323–335. https://doi.org/10.1016/J.MATDES.2012.08.056.

Wang, Q., Hussain, A., Farooqi, M.U., Deifalla, A.F., 2022. Artificial intelligence-based estimation of ultra-high-strength concrete's flexural property. Case Stud. Constr. Mater. 17, e01243 https://doi.org/10.1016/j.cscm.2022.e01243.

Willmott, Cort J., Matsuura, Kenji, 2005. Advantages of the mean absolute error (MAE) over the root mean square error (RMSE) in assessing average model performance. Clim. Res. 30, 79–82.

World Health Organization, 2009. WHO Handbook on Indoor Radon (Geneva, Switzerland).

Xhixha, G., Bezzon, G.P., Broggini, C., Buso, G.P., Caciolli, A., Callegari, I., de Bianchi, S., Fiorentini, G., Guastaldi, E., Kaçeli Xhixha, M., Mantovani, F., Massa, G., Menegazzo, R., Mou, L., Pasquini, A., Alvarez, C.R., Shyti, M., 2013. The worldwide NORM production and a fully automated gamma-ray spectrometer for their characterization. J. Radioanal. Nucl. Chem. 295, 445–457. https://doi.org/10.1007/s10967-012-1791-1.

Xu, J., Zhao, X., Yu, Y., Xie, T., Yang, G., Xue, J., 2019. Parametric sensitivity analysis and modelling of mechanical properties of normal- and high-strength recycled aggregate concrete using grey theory, multiple nonlinear regression and artificial neural networks. Construct. Build. Mater. 211, 479–491. https://doi.org/10.1016/j.conbuildmat.2019.03.234.

Yeh, I.-C., 1998. Modeling of strength of high-performance concrete using artificial neural networks. Cement Concr. Res. 28, 1797–1808. https://doi.org/10.1016/S0008-8846(98)00165-3.

Yu, Q., 1996. Investigation on the radioactivity concentration of coal and ash from Shanghai coal-fired power plant, China. J. Radiol. Med. Prot 16, 374–375.

Zak, A., I, K., P, B., K, M., Z, A., S, T., 2008. Natural radioactivity of wastes. Nukleonika 55, 387–391.

Zeller, B., 1995. Radioaktivitätsbilanzen in Steinkohlekraftwerken, Diplomarbeit im FB Technisches Gesundheitswesen. FIZ Gießen–Friedberg.

Ziolkowski, P., Niedostatkiewicz, M., 2019. Machine learning techniques in concrete mix design. Materials 12, 1256. https://doi.org/10.3390/ma12081256.